

Table of Content

GENERAL METHODS FOR SYNTHESIS	S2
INSTRUMENTS	S2
SYNTHESIS	S3
X-RAY STRUCTURE OF <i>LINEAR</i> -DITT (CCDC: 2159650)	S11
X-RAY STRUCTURE OF <i>ANTI</i> -DITT (CCDC: 2159651)	S12
X-RAY STRUCTURE OF <i>SYN</i> -DITT (CCDC: 2159652).....	S13
X-RAY STRUCTURE OF <i>LINEAR</i> -IF (CCDC: 2159653).....	S14
CYCLIC VOLTAMMETRY DATA	S15
EXPERIMENTAL AND CALCULATED BOND LENGTHS COMPARISON	S16
THEORITICAL CALCULATIONS	S17
OFETs.....	S21
RMN SPECTRA	S24
INFRARED SPECTRA	S32
REFERENCES	S34

GENERAL METHODS FOR SYNTHESIS

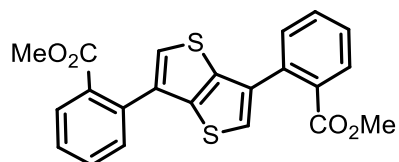
All reactions were carried out under argon. Dichloromethane was distilled from P₂O₅, THF and Toluene were distilled over Na/benzophenone. Dichloromethane and Toluene were kept over activated 3 Å molecular sieves. All commercial reagents were used without further purification. 4,9-dibromo-1,2,3,6,7,8-hexahydropyrene, ⁱ methyl 2-(4,4,5,5-tetramethyl-1,3,2-dioxaborolan-2-yl)benzoate, ⁱⁱ methyl 1-(4,4,5,5-tetramethyl-1,3,2-dioxaborolan-2-yl)-2-naphthoate, ⁱⁱⁱ 3-(4,4,5,5-tetramethyl-1,3,2-dioxaborolan-2-yl)-2-naphthoate, ^{iv} and methyl 3-(4,4,5,5-tetramethyl-1,3,2-dioxaborolan-2-yl)-2-naphthoate,^v were obtained according to procedures described from literature. ¹H and ¹³C NMR spectra were recorded at room temperature on Bruker Avance-300 MHz NMR spectrometer. ¹H NMR spectra were recorded at 300 MHz and ¹³C NMR spectra were recorded at 75 MHz. Chloroform residual peak was taken as internal reference at 7.26 ppm for ¹H NMR and 77 ppm for ¹³C NMR. *o*-Dichlorobenzene-D₄ residual peak was taken as internal reference at 7.20 ppm for ¹H NMR. Toluene-D₈ was taken as internal reference at 7.25 ppm for ¹H NMR. Infrared spectra were recorded from Nicolet 6700 FT-IR spectrometer. High-resolution mass spectra were obtained by using Waters Xevo Q-ToF using positive mode. MALDI High-resolution mass spectra and Elementary analysis were performed by the analysis platform of ICSN (Centre de Recherche de Gif - www.icsn.cnrs-gif.fr).

INSTRUMENTS

Cyclic voltammetry was performed with BAS Electrochemical system in a three-electrode single-compartment cell with a glassy carbon working electrode, a coiled platinum wire counter electrode, and an Ag/AgNO₃ reference electrode. The measurements were carried out in dry chlorobenzene using a 0.1 M tetrabutylammonium hexafluorophosphate (TBAPF₆) electrolyte, the solution being purged with nitrogen prior to measurement. All potentials were internally referred to the ferrocene/ferrocenium couple. Ultraviolet-visible (UV-vis) absorption spectra were recorded on UV-vis (Lambda 950-PKA, PerkinElmer) spectrophotometer. The channel width and length were measured optically with a laser scanning microscope (Olympus LEXT).

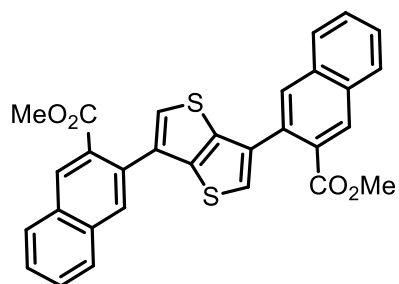
SYNTHESIS

Compound 1a



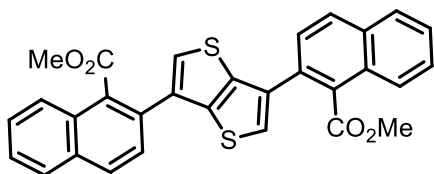
A solution of 3,6-dibromothiopheno[3,2-*b*]thiophene (1 g, 3.36 mmol), methyl 2-(4,4,5,5-tetramethyl-1,3,2-dioxaborolan-2-yl)benzoate (2.64 g, 10.01 mmol), K_3PO_4 (4.27 g, 20.14 mmol) and toluene/water (39/4 mL) was degassed for 30 min with argon. Tris(dibenzylideneacetone)dipalladium (0) ($Pd_2(dba)_3$) (154 mg; 0.17 mmol) and S-Phos (138 mg; 0.34 mmol) were then added. The resulting solution was heated at 100°C for 36 hours. The crude mixture was left to return to room temperature and then diluted with chloroform. The solution was filtered through a pad of silica gel with chloroform. The resulting solution was concentrated under vacuum. The crude product was precipitated in DCM/MeOH twice. The resulting solid was then washed quickly with cold dichloromethane to afford compound **1a** as white solid (1.08 g, 79%). 1H NMR (300 MHz, $CDCl_3$) δ 7.95 – 7.87 (m, 2H), 7.66 – 7.56 (m, 4H), 7.52 – 7.45 (m, 2H), 7.27 (d, $J = 4.4$ Hz, 2H), 3.69 (s, 6H); ^{13}C NMR (75 MHz, $CDCl_3$) δ 168.50, 139.30, 135.17, 134.13, 131.72, 130.95, 130.39, 130.22, 128.01, 123.75, 52.25; HRMS (ESI+): calculated for $C_{22}H_{16}O_4S_2+H^+$ ($M+H$) $^+$: 409.0568; found: 409.0555; mass error: -3.2 ppm.

Compound 1b



The same experimental protocol of compound **1a** was used with :
3,6-dibromothiopheno[3,2-*b*]thiophene (1 g, 3.36 mmol).
methyl 3-(4,4,5,5-tetramethyl-1,3,2-dioxaborolan-2-yl)-2-naphthoate (3.15 g, 10.01 mmol).
 K_3PO_4 (4.27 g, 20.14 mmol), ($Pd_2(dba)_3$) (154 mg; 0.17 mmol), S-Phos (138 mg; 0.34 mmol).
Toluene/water (39/4 mL).
white solid (1.41 g, 83%). 1H NMR (300 MHz, $CDCl_3$) δ 8.49 (s, 2H), 8.09 (s, 2H), 7.98 (d, $J = 7.6$ Hz, 2H), 7.91 (d, $J = 7.6$ Hz, 2H), 7.67 – 7.55 (m, 4H), 7.33 (s, 2H), 3.75 (s, 6H); ^{13}C NMR (75 MHz, $CDCl_3$) δ 168.39, 139.58, 134.51, 134.46, 131.98, 131.58, 131.55, 129.77, 128.74, 128.70, 128.48, 127.84, 127.11, 123.57, 52.37; HRMS (ESI+): calculated for $C_{30}H_{20}O_4S_2+Na^+$ ($M+Na$) $^+$: 531.0701; found: 531.0708; mass error: 1.3 ppm.

Compound 1c



The same experimental protocol of compound **1a** was used with :

3,6-dibromothieno[3,2-*b*]thiophene (1 g, 3.36 mmol).

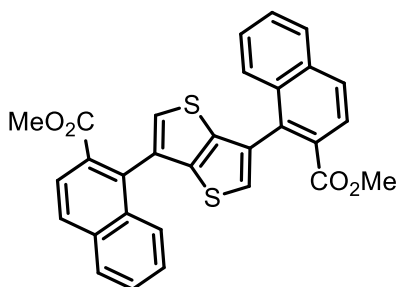
methyl 2-(4,4,5,5-tetramethyl-1,3,2-dioxaborolan-2-yl)benzoate (3.15 g, 10.01 mmol).

K₃PO₄ (4.27 g, 20.14 mmol), (Pd₂(dba)₃) (154 mg; 0.17 mmol), S-Phos (138 mg; 0.34 mmol).

Toluene/water (39/4 mL).

White solid (1.51 g, 88%); ¹H NMR (300 MHz, CDCl₃) δ 8.04 (d, *J* = 8.6 Hz, 2H), 7.93 (d, *J* = 8.1 Hz, 4H), 7.84 (d, *J* = 8.5 Hz, 2H), 7.65 – 7.54 (m, 4H), 7.47 (s, 2H), 3.84 (s, 6H); ¹³C NMR (75 MHz, CDCl₃) δ 169.94, 133.24, 132.68, 130.50, 130.32, 130.15, 128.25, 127.70, 126.73, 125.55, 125.16, 124.89, 52.58; HRMS (ESI⁺): calculated for C₃₀H₂₀O₄S₂+Na⁺ (*M*+Na)⁺: 531.0701; found: 531.0708; mass error: 1.3 ppm.

Compound 1d



The same experimental protocol of compound **1a** was used with :

3,6-dibromothieno[3,2-*b*]thiophene (1 g, 3.36 mmol).

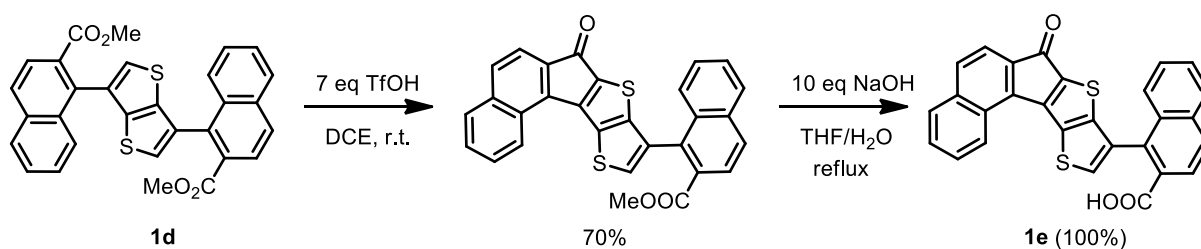
methyl 1-(4,4,5,5-tetramethyl-1,3,2-dioxaborolan-2-yl)-2-naphthoate (3.15 g, 10.01 mmol).

K₃PO₄ (4.27 g, 20.14 mmol), (Pd₂(dba)₃) (154 mg; 0.17 mmol), S-Phos (138 mg; 0.34 mmol).

Toluene/water (39/4 mL).

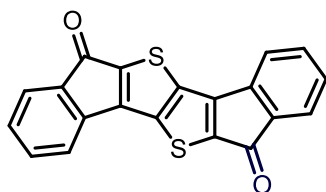
Two rotamers were obtained as White solid (1.66 g, 96%); ¹H NMR (300 MHz, CDCl₃) δ 8.11 – 7.89 (m, 7H), 7.83 (d, *J* = 8.5 Hz, 0.79H), 7.71 – 7.45 (m, 4H), 7.27 (d, *J* = 2.3 Hz, 2H), 3.70 (s, 2.48H), 3.69 (s, 3.52H); ¹³C NMR (75 MHz, CDCl₃) δ 168.50, 168.46, 140.74, 140.67, 134.89, 134.87, 134.17, 134.07, 132.34, 132.30, 131.34, 131.27, 129.43, 129.17, 128.70, 128.67, 128.14, 127.83, 127.81, 127.37, 127.27, 127.02, 125.69, 125.46, 125.32, 52.21; HRMS (ESI⁺): calculated for C₃₀H₂₀O₄S₂+Na⁺ (*M*+Na)⁺: 531.0701; found: 531.0700; mass error: -0.2 ppm.

Compound 1e



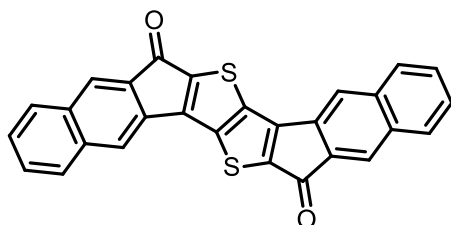
Compound **1d** (1.08 g, 2.11 mmol) was dissolved in 1,2-dichloroethane (60 mL) under inert atmosphere. TfOH (1.31 mL, 14.83 mmol) was then added dropwise. The resulting mixture was then stirred at room temperature for 7 hours. Saturated aqueous NaHCO₃ was added to the mixture solution until neutral pH. The mixture was extracted three times with chloroform. The combined organic phase was washed twice with water. After drying with magnesium sulfate and concentrated under vacuum, the crude product was filtered over a pad of silica gel using a mixture (chloroform/ethyl acetate; 100/0 to 100/1) as eluent to give the targeted molecule as yellow solid (703 mg, 70%). Then, to a solution of the intermediate (703 mg, 1.48 mmol) in THF (60 mL), was added a solution of NaOH (590 mg, 14.75 mmol) in water (30 mL) and then stirred at 85°C for 4h. After allowing the mixture to cool down to room temperature, the mixture was diluted with water and acidified with concentrated aqueous HCl. The resulting precipitate was filtered and washed with water. The precipitate was dried under vacuum to afford compound **1e** as yellow solid (572 mg, quant). ¹H NMR (300 MHz, DMSO) δ 13.10 (s, 1H), 8.41 (d, *J* = 8.4 Hz, 1H), 8.23 (d, *J* = 8.6 Hz, 1H), 8.17 (d, *J* = 6.8 Hz, 2H), 8.04 (d, *J* = 8.6 Hz, 1H), 7.99 (d, *J* = 8.3 Hz, 1H), 7.89 (d, *J* = 8.1 Hz, 1H), 7.80-7.60 (m, 5H), 7.56 (d, *J* = 8.1 Hz, 1H); ¹³C NMR (75 MHz, DMSO) δ 187.54 (CO, 5-membered ring), 169.97, 154.34, 150.60, 139.07, 139.00, 137.71, 136.02, 134.98, 134.37, 134.08, 133.53, 133.02, 133.00, 131.99, 131.30, 131.08, 130.19, 130.07, 129.80, 129.46, 127.88, 127.53, 127.49, 125.94, 121.48. HRMS (ESI⁺): calculated for C₂₈H₁₄O₃S₂+H⁺ (*M*+H)⁺: 463.0463; found: 463.0464; mass error: 0.2 ppm.

Compound 2a



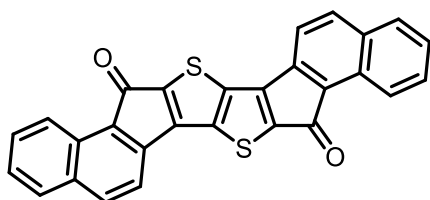
Compound **1a** (1.04 g, 2.55 mmol) was put in suspension in 1,2-dichloroethane (50 mL). TfOH (12.5 mL, 252 mmol) was then added dropwise. The resulting mixture is stirred at 80°C for 7 hours. After allowing the reaction mixture to cool down to room temperature, the mixture was transferred to an Erlenmeyer flask with chloroform and a saturated aqueous NaHCO₃ solution was added until neutral pH, followed by methanol and water to obtain one phase. The resulting precipitate is filtered, washed with water, MeOH prior to drying under vacuum to afford compound **2a** as red solid. (764 mg, 87%). Due to the insolubility of the compound, no NMR measurements could be recorded. Elementary analysis calculated for C₂₀H₈O₂S₂: %C: 69.75; %H: 2.34; %S: 18.62; found for %C: 69.54; %H: 2.10; %S: 18.98. IR (cm⁻¹): 1692 (C=O stretching of 5-membered ring).

Compound 2b



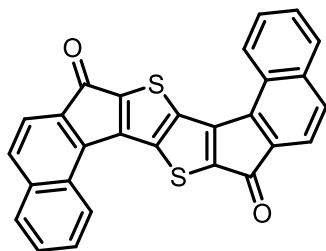
Compound **1b** (0.600 g, 1.18 mmol) was put in suspension in 1,2-dichloroethane (50 mL) TfOH (8.85 mL, 59 mmol) was then added dropwise. The resulting mixture was stirred overnight at room temperature. The mixture was transferred to an Erlenmeyer flask with chloroform and a saturated aqueous NaHCO₃ solution was added until neutral pH, followed by methanol and water to obtain one phase. The resulting precipitate is filtered, washed with water, MeOH and petroleum ether several time before drying under vacuum to afford compound **2b** as red solid (480 mg, 91%). Due to the insolubility of the compound, no NMR measurements could be recorded. Elementary analysis calculated for C₂₈H₁₂O₂S₂: %C: 75.65; %H: 2.72; %S: 14.43; found for %C: 75.40; %H: 2.94; %S: 14.66. IR (cm⁻¹): 1693 (C=O stretching of 5-membered ring).

Compound 2c



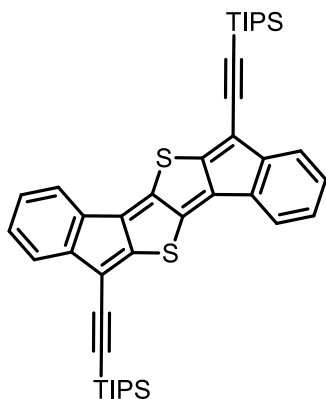
Compound **1c** (0.87 g, 1.71 mmol) was put in suspension in 1,2-dichloroethane (60 mL). TfOH (7.55 mL, 85 mmol) was then added dropwise. The resulting mixture was stirred for 10 min at room temperature. The mixture was transferred to an Erlenmeyer flask with chloroform and a saturated aqueous NaHCO₃ solution was added until neutral pH, followed by methanol and water to obtain one phase. The resulting precipitate is filtered, washed with water, MeOH and petroleum ether several time before drying under vacuum to afford compound **6** as green solid (743 mg, 98%) Due to the insolubility of the compound, no NMR measurements could be recorded. Elementary analysis calculated for C₂₈H₁₂O₂S₂: %C: 75.65; %H: 2.72; %S: 14.43; found for %C: 75.44; %H: 2.90; %S: 14.60. IR (cm⁻¹): 1690 (C=O stretching of 5-membered ring).

Compound 2d



To a suspension of compound **1e** (601 mg, 1.30 mmol) in dichloromethane (120 mL), was added oxalyl chloride (0.145 mL, 1.69 mmol) and then DMF (8.05 μ L, 0.1 mmol). The resulting mixture was stirred for 3h at room temperature and turned to a red solution. The obtained acyl-chloride was dried under vacuum to remove dichloromethane and remaining oxalyl chloride. The resulting mixture is solubilised with dichloromethane (120 mL) and then AlCl_3 (480 mg, 3,6 mmol) was added in one portion. After stirring overnight at room temperature, the resulting solution is quenched with a mixture of MeOH (220 mL) and concentrated aqueous HCl (20 mL). The resulting precipitate is filtered, washed with MeOH, water and MeOH again before drying under vacuum to afford compound **10** as dark yellow solid (455 mg, 79%). % Due to the insolubility of the compound, no NMR measurements could be recorded. Elementary analysis calculated for $\text{C}_{28}\text{H}_{12}\text{O}_2\text{S}_2$: %C: 75.65; %H: 2.72; %S: 14.43; found for %C: 75.38; %H: 2.88; %S: 14.62. IR (cm^{-1}): 1699 (CO stretching of 5-membered ring).

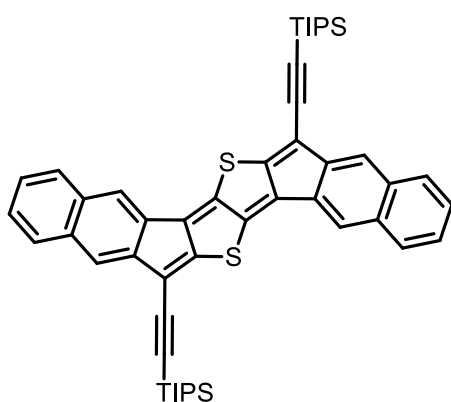
DITT



To a stirred suspension of compound **2a** (367 mg, 1.07 mmol) in THF (120 mL) at 0°C is added a solution of TIPS-lithium acetylide (6 mmol) in THF (20 mL) under argon. The resulting mixture is stirred and left to return to room temperature for 2 hours. Then, the resulting mixture is quenched with aqueous solution of NH_4Cl and extracted several times with diethyl ether. The organic phases are washed with water twice, dried over magnesium sulfate and concentrated under vacuum at a temperature lower than 40°C. The crude product was precipitated with petroleum ether to remove the excess of TIPS-acetylene. Due to the instability of the compound, it was directly used without further purification (602 mg, 77%). The diol was solubilized in toluene (70 mL) and the mixture was degassed for 30 min with argon. Then, SnCl_2 (624 mg, 3.29 mmol) was added in one portion. The mixture was stirred for 2h30 at

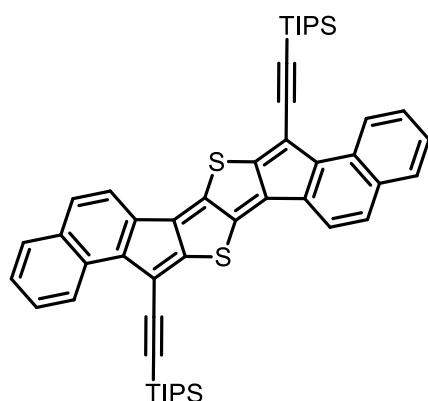
room temperature and then filtered over of pad of silica gel (toluene). The filtrate was concentrated under vacuum. The solid was precipitated in a dichloromethane/acetonitrile mixture, filtered and washed with acetonitrile and methanol. This precipitation/washing process is repeated twice. Then, the powder is dried under vacuum to give **DITT** as blue solid (489 mg, 67%) (global yield over two steps 52%). Due to the low solubility of the molecule, ^{13}C NMR couldn't be recorded. ^1H NMR (300 MHz, CDCl_3) δ 7.32 (d, $J = 7.2$ Hz, 2H), 7.22 – 7.15 (m, 4H), 7.07 (td, $J = 7.2, 2.3$ Hz, 2H), 1.18 (s, 42H); ^{13}C NMR (75 MHz, CDCl_3) δ 150.08, 147.27, 146.92, 139.37, 129.56, 128.76, 125.47, 122.61, 120.68, 114.70, 105.37, 99.94, 18.74, 11.26. HRMS (MALDI-TOF): calculated for $\text{C}_{42}\text{H}_{50}\text{S}_2\text{Si}_2$ (M^+): 674.28870; found: 674.29176, mass error: 4.5 ppm.

linear-DITT



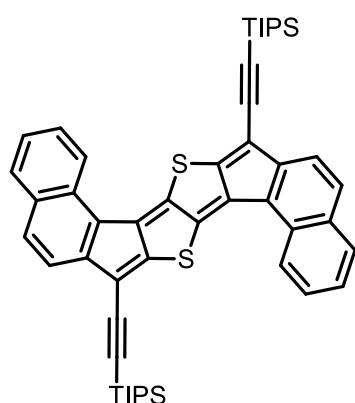
To a stirred suspension of compound **2b** (300 mg, 0.67 mmol) in THF (120 mL) at 0°C is added a solution of TIPS-lithium acetylide (4.05 mmol) in THF (15 mL) under argon. The resulting mixture is stirred and left to return to room temperature for 2 hours. Then, the resulting mixture is quenched with aqueous NH_4Cl and extracted several times with diethyl ether. The organic phases are washed with water twice, dried over magnesium sulfate and concentrated under vacuum at a temperature lower than 40°C. The crude product was precipitated with petroleum ether to remove the excess of TIPS-acetylene. Due to the instability of the compound, it was directly used without further purification (448 mg, 82%). The diol was solubilized in toluene (64 mL) and the mixture was degassed for 30 min with argon. Then, SnCl_2 (420 mg, 2.21 mmol) was added in one portion. The mixture was stirred for 15h at room temperature and then filtered over of pad of silica gel (toluene). The filtrate was concentrated under vacuum. The solid was precipitated in a dichloromethane/acetonitrile mixture, filtered and washed with acetonitrile and methanol. This precipitation/washing process is repeated twice. Then the compound is precipitated in a dichloromethane/petroleum ether mixture. After removal of the dichloromethane under vacuum, the precipitate is filtrated and washed with petroleum ether. The powder is dried under vacuum to give *linear-DITT* as blue solid (317 mg, 74%) (global yield over two steps 61%). Due to the low solubility of the molecule, ^{13}C NMR couldn't be recorded. ^1H NMR (300 MHz, CDCl_3) δ 7.86 – 7.81 (m, 2H), 7.79 – 7.73 (m, 4H), 7.57 (s, 2H), 7.46 – 7.40 (m, 4H), 1.24 (s, 42H). HRMS (MALDI-TOF): calculated for $\text{C}_{50}\text{H}_{54}\text{S}_2\text{Si}_2$ (M^+): 774.32000; found: 774.31997, mass error: -0.04 ppm.

***anti*-DITT**



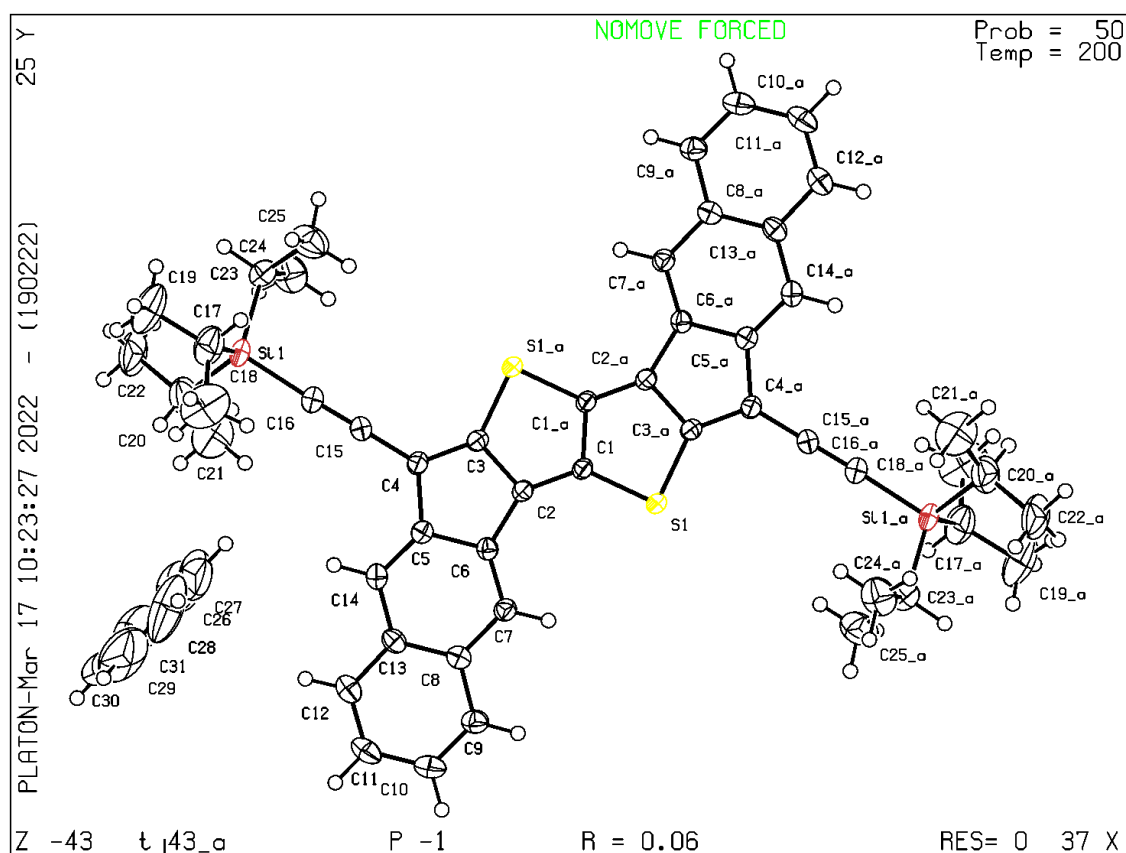
To a stirred suspension of compound **2c** (310 mg, 0.70 mmol) in THF (120 mL) at 0°C is added a solution of TIPS-lithium acetylide (4.18 mmol) in THF (15 mL) under argon. The resulting mixture is stirred and left to return to room temperature for 2 hours. Then, the resulting mixture is quenched with aqueous NH₄Cl and extracted several times with diethyl ether. The organic phases are washed with water twice, dried over magnesium sulfate and concentrated under vacuum at a temperature lower than 40°C. The crude product was precipitated with petroleum ether to remove the excess of TIPS-acetylene. Due to the instability of the compound, it was directly used without further purification (440 mg, 78%). The diol was solubilized in toluene (60 mL) and the mixture was degassed for 30 min with argon. Then, SnCl₂ (413 mg, 2.18 mmol) was added in one portion. The mixture was stirred for 15h at room temperature and then filtered over of pad of silica gel (toluene). The filtrate was concentrated under vacuum. The solid was precipitated in a dichloromethane/acetonitrile mixture, filtered and washed with acetonitrile and methanol. This precipitation/washing process is repeated twice. Then the compound is precipitated in a dichloromethane/petroleum ether mixture. After removal of the dichloromethane under vacuum, the precipitate is filtrated and washed with petroleum ether. The powder is dried under vacuum to give ***anti*-DITT** (287 mg, 68%) (global yield over two steps 53%). Due to the low solubility of the molecule, ¹³C NMR couldn't be recorded. ¹H NMR (300 MHz, Tol) δ 9.51 (d, *J* = 8.2 Hz, 2H), 7.72 (d, *J* = 8.3 Hz, 2H), 7.53 (d, *J* = 7.4 Hz, H), 7.48 (d, *J* = 8.3 Hz, 2H), 7.41-7.37 (m, 4H), 1.52 (s, 42H). HRMS (MALDI-TOF): calculated for C₅₀H₅₄S₂Si₂ (*M*⁺): 774.32000; found: 774.31903; mass error: -1.3 ppm.

syn-DITT



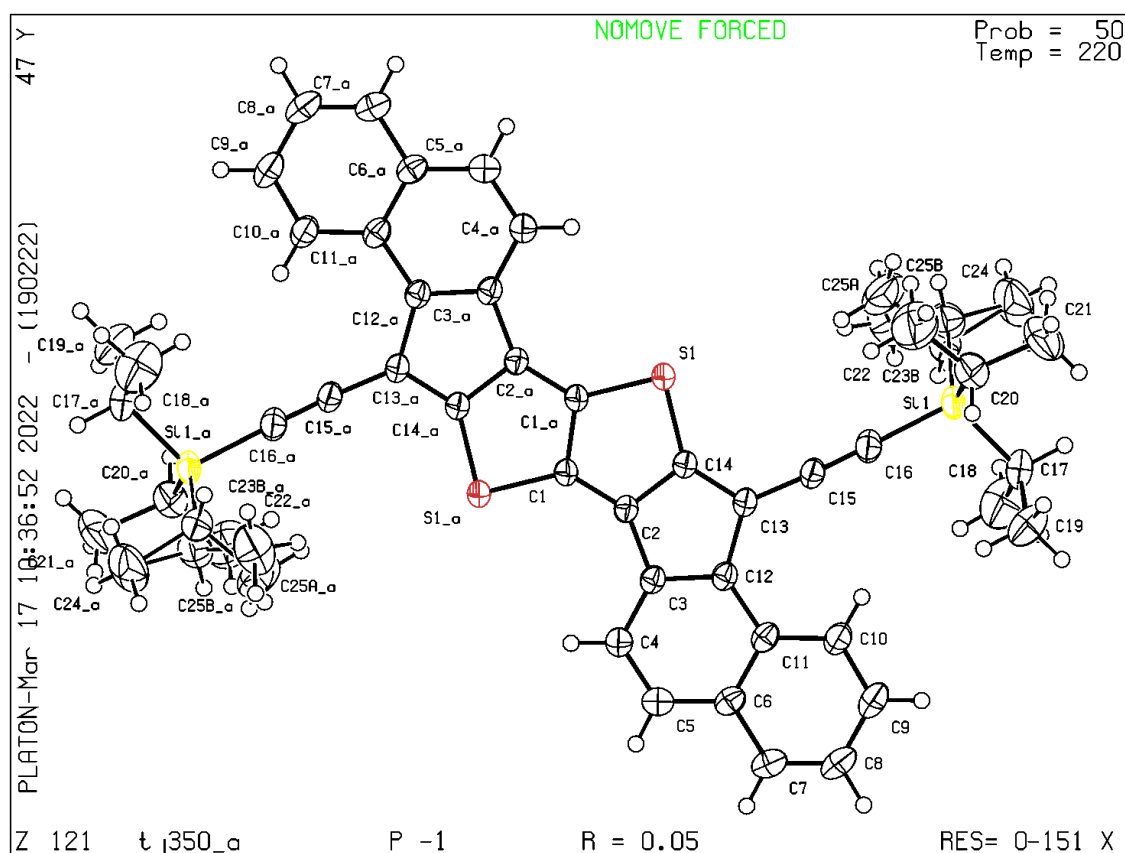
To a stirred suspension of compound **2d** (200 mg, 0.45 mmol) in THF (80 mL) at 0°C is added a solution of TIPS-lithium acetylide (2.70 mmol) in THF (10 mL) under argon. The resulting mixture is stirred and left to return to room temperature for 2 hours. Then, the resulting mixture is quenched with aqueous NH₄Cl and extracted several times with diethyl ether. The organic phases are washed with water twice, dried over magnesium sulfate and concentrated under vacuum at a temperature lower than 40°C. The crude product was precipitated with petroleum ether to remove the excess of TIPS-acetylene. Due to the instability of the compound, it was directly used without further purification (364 mg, 82%). The diol was solubilized in toluene (50 mL) and the mixture was degassed for 30 min with argon. Then, SnCl₂ (341 mg, 1.80 mmol) was added in one portion. The mixture was stirred for 1h30 at room temperature and then filtered over of pad of silica gel (toluene). The filtrate was concentrated under vacuum. The solid was precipitated in a dichloromethane/acetonitrile mixture, filtered and washed with acetonitrile and methanol. This precipitation/washing process is repeated twice. Then the compound is precipitated in a dichloromethane/petroleum ether mixture. After removal of the dichloromethane under vacuum, the precipitate is filtrated and washed with petroleum ether. The powder is dried under vacuum to give *syn*-DITT as purple solid (80 mg, 23%) (global yield over two steps 19%). Due to the low solubility of the molecule, ¹³C NMR couldn't be recorded. ¹H NMR (300 MHz, *o*-C₆D₄Cl₂) δ 8.14 (d, *J* = 8.5 Hz, 2H), 7.62 (d, *J* = 8.2 Hz, 2H), 7.56 (d, *J* = 8.3 Hz, 2H), 7.45-7.39 (m, 4H), 7.25 (s, 2H), 1.32 – 1.02 (m, 42H). HRMS (MALDI-TOF): calculated for C₅₀H₅₄S₂Si₂ (*M*⁺): 774.32000; found: 774.31722; mass error: -3.6 ppm.

X-RAY STRUCTURE OF *LINEAR-DITT* (CCDC: 2159650)



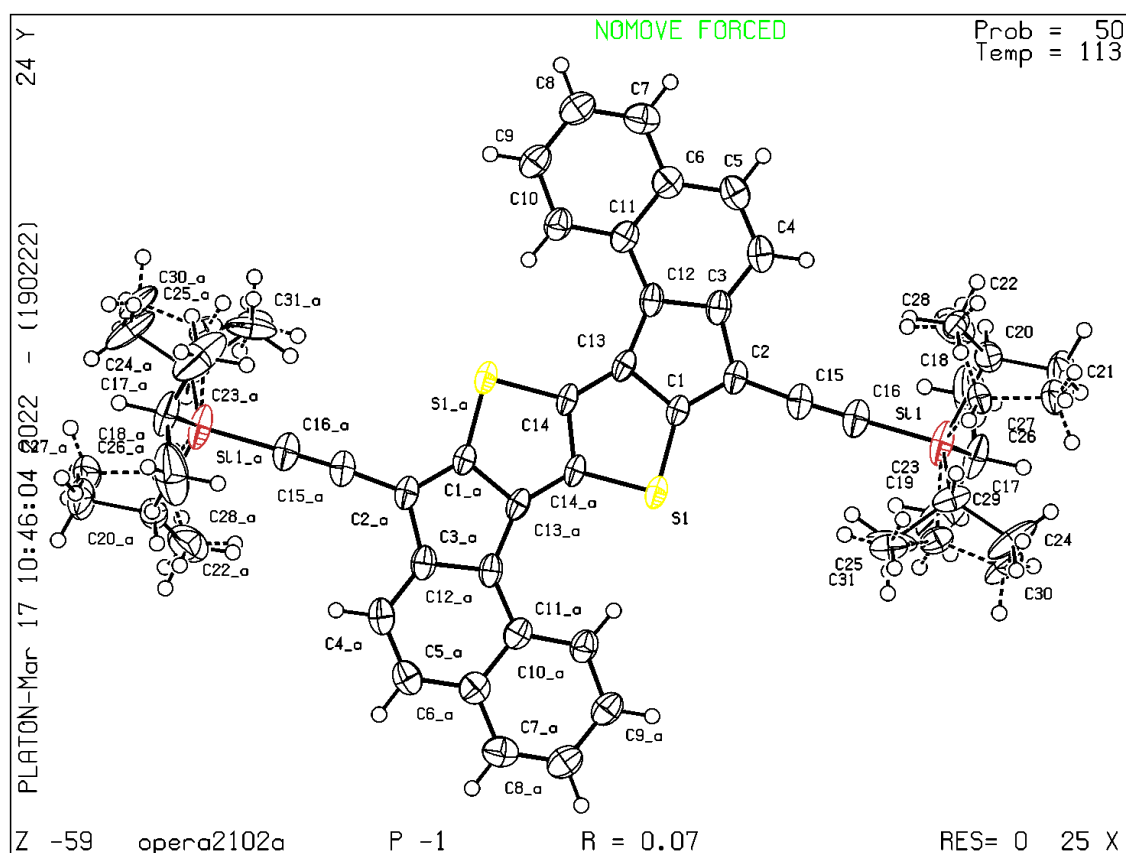
Crystal data for *linear-DITT* (+ 2 benzene): $C_{62}H_{66}S_2Si_2$, $M_w = 931.44$, , triclinic, space group P-1; dimensions: $a = 9.0054(5) \text{ \AA}$, $b = 9.2181(4) \text{ \AA}$, $c = 16.4615(8) \text{ \AA}$, $\alpha = 96.538(2)^\circ$, $\beta = 97.301(2)^\circ$, $\gamma = 96.091(2)^\circ$, $V = 1336.50(11) \text{ \AA}^3$; $Z = 1$; $\mu = 0.18 \text{ mm}^{-1}$; 42031 reflections measured at 200 K; independent reflections: 4727 [$4087 F_o > 4\sigma(F_o)$]; data were collected up to a $2\theta_{max}$ value of 50.1° (99.8 % coverage). Number of variables: 292; $R_1 = 0.061$, $wR_2 = 0.164$, $S = 1.02$; highest residual electron density 1.01 e.\AA^{-3} ; CCDC = 2159650.

X-RAY STRUCTURE OF ANTI-DITT (CCDC: 2159651)



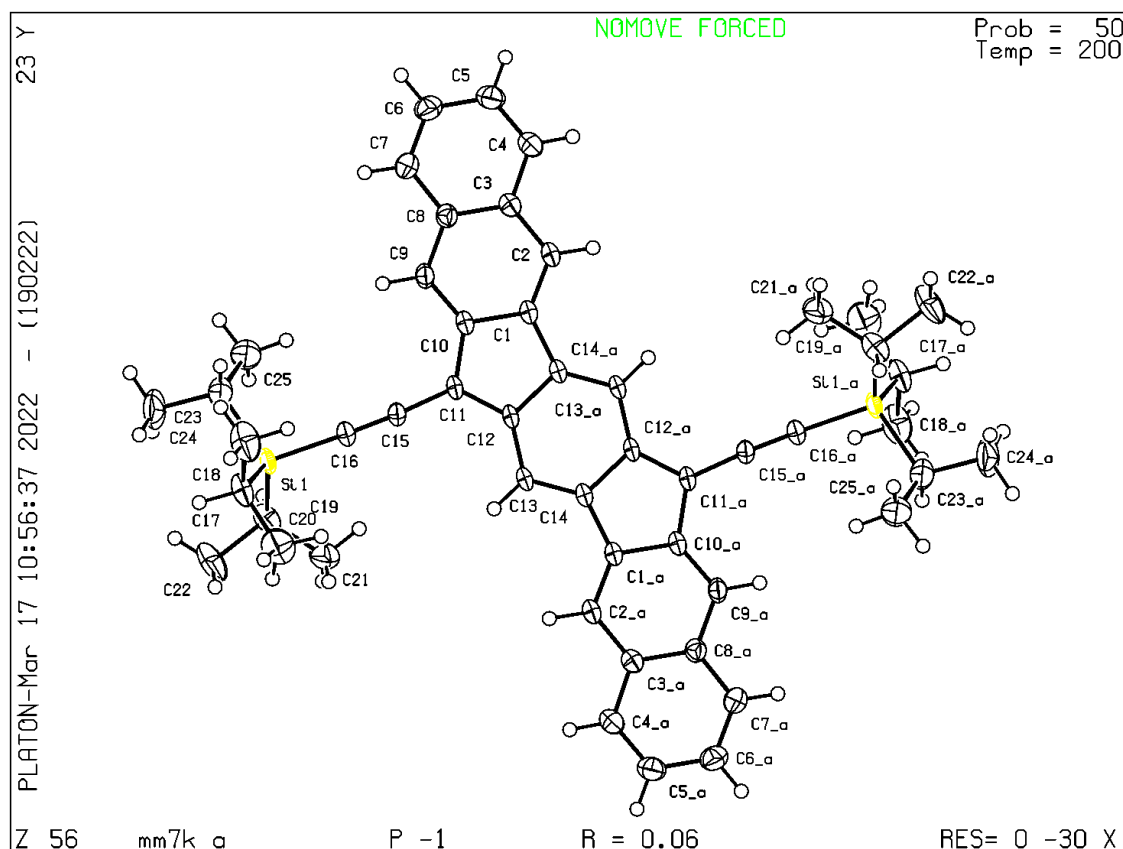
Crystal data for *anti*-DITT : C₅₀H₅₄S₂Si₂, M_w = 775.23, triclinic, space group P-1; dimensions: a = 7.7487(3) Å, b = 8.6569(4) Å, c = 16.4606(8) Å, α = 82.696(2)°, β = 89.654(2)°, γ = 84.504(2)°, V = 1090.16(8) Å³; Z = 1; μ = 0.21 mm⁻¹; 47975 reflections measured at 220 K; independent reflections: 6336 [5329 Fo > 4σ(Fo)]; data were collected up to a 2θ_{max} value of 60.0° (99.9 % coverage). Number of variables: 269; R₁ = 0.049, wR₂ = 0.126, S = 1.06; highest residual electron density 0.91 e.Å⁻³; CCDC = 2159651.

X-RAY STRUCTURE OF *syn*-DITT (CCDC: 2159652)



Crystal data for *syn*-DITT : $C_{50}H_{54}S_2Si_2$, $M_w = 775.23$, triclinic, space group P-1; dimensions: $a = 7.9845(5)$ Å, $b = 10.8188(7)$ Å, $c = 13.4966(8)$ Å, $\alpha = 113.020(6)^\circ$, $\beta = 98.401(5)^\circ$, $\gamma = 93.099(5)^\circ$, $V = 1053.57(12)$ Å³; $Z = 1$; $\mu = 0.22$ mm⁻¹; 17449 reflections measured at 113 K; independent reflections: 4825 [3132 $F_o > 4\sigma(F_o)$]; data were collected up to a $2\theta_{max}$ value of 54.97° (99.8 % coverage). Number of variables: 309; $R_1 = 0.068$, $wR_2 = 0.181$, $S = 1.02$; highest residual electron density 0.47 e.Å⁻³; CCDC = 2159652.

X-RAY STRUCTURE OF *LINEAR-IF* (CCDC: 2159653)



Crystal data for *linear-IF*: C₅₀H₅₆Si₂, M_w = 713.12, triclinic, space group P-1; dimensions: a = 8.5267(5) Å, b = 10.9050(6) Å, c = 12.0689(6) Å, α = 109.615(2)°, β = 98.164(2)°, γ = 90.789(3)°, V = 1044.1(1) Å³; Z = 1; μ = 0.12 mm⁻¹; 43801 reflections measured at 200 K; independent reflections: 6091 [4825 Fo > 4σ(Fo)]; data were collected up to a 2θ_{max} value of 60.1° (99.9 % coverage). Number of variables: 241; R₁ = 0.057, wR₂ = 0.169, S = 1.04; highest residual electron density 1.06 e.Å⁻³; CCDC = 2159653.

CYCLIC VOLTAMMETRY DATA

Cyclic voltammetry was performed with BAS Electrochemical system in a three-electrode single-compartment cell with a glassy carbon working electrode, a coiled platinum wire counter electrode, and an Ag/AgNO₃ reference electrode. Cyclic voltammetry was recorded using 1-2 mM in 0.1 M Bu₄N.PF₆ /chlorobenzene using a scan rate of 100 mV s⁻¹. Energy level was determined by $E_{\text{LUMO}} = -(4.8 + E_{\text{red1}}^{\text{ons}})$ and $E_{\text{HOMO}} = -(4.8 + E_{\text{ox1}}^{\text{ons}})$. The optical HOMO-LUMO energy gap ($E_{\text{gap}}^{\text{opt}}$) was determined as the intersection of the x-axis and a tangent line that passes through the inflection point of the lowest energy absorption.

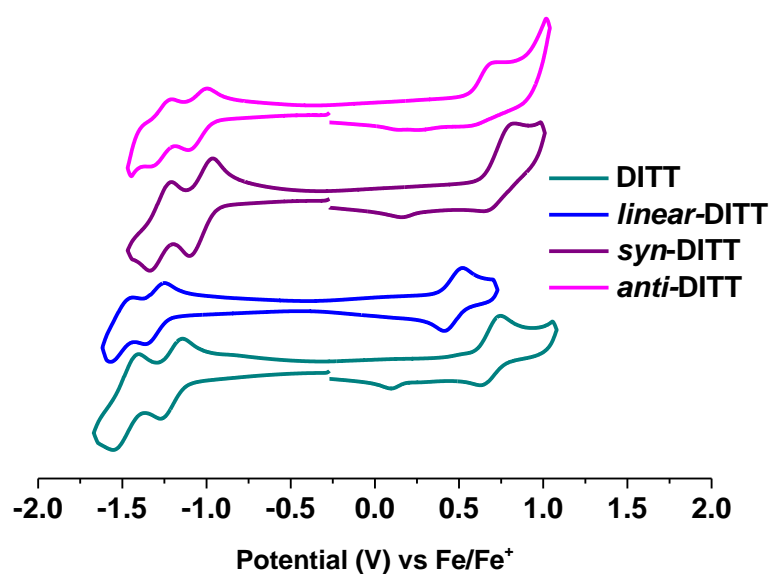


Table S1.

compounds	$E_{\text{ox}}^{\text{ons}}$ (V)	$E_{\text{red1}}^{1/2} / E_{\text{red1}}^{\text{ons}}$ (V)	$E_{\text{red2}}^{1/2}$ (V)	HOMO (eV)	LUMO (eV)	$E_{\text{gap}}^{\text{elec}}$ (eV)	$E_{\text{gap}}^{\text{opt}}$ (eV)
DITT	0.60	-1.21 / -1.12	-1.49	-5.40	-3.68	1.72	1.59
linear-DITT	0.39	-1.31 / -1.23	-1.51	-5.19	-3.57	1.62	1.69
syn-DITT	0.63	-1.04 / -0.94	-1.28	-5.43	-3.86	1.57	1.38
anti-DITT	0.56	-1.05 / -0.98	-1.27	-5.36	-3.82	1.54	1.30

EXPERIMENTAL AND CALCULATED BOND LENGTHS COMPARISON

Table S2.

Compounds	Bond a/b experimental	Bond a/b calculated	R factor (%)	y_0
DITT	1.486 (5) / 1.372 (5) ^[a] 1.482 (6) / 1.369 (6) ^[b]	1.484 / 1.374	5.3 7.2	7
<i>linear</i> -DITT	1.480 (4) / 1.365 (4)	1.477 / 1.377	6.1	7
<i>syn</i> -DITT	1.469 (4) / 1.362 (4)	1.480 / 1.368	6.8	15
<i>anti</i> -DITT	1.490 (2) / 1.370 (2)	1.493 / 1.374	4.9	15
IF	1.472 (6) / 1.382 (6) ^[c]	1.467 / 1.395	8.2	40
<i>linear</i> -IF	1.472 (4) / 1.399 (4) ^[d] 1.455 (2) / 1.397 (2)	1.463 / 1.395	6.3 5.7	43
<i>syn</i> -IF	1.469 (5) / 1.377 (4) ^[d]	1.459 / 1.396	6.3	46
<i>anti</i> -IF	1.465 (3) / 1.401 (3) ^[d]	1.463 / 1.404	4.8	50
HDIP	1.454 (2) / 1.406 (2) ^[e]	1.455 / 1.409	4.5	56
<i>linear</i> -HDIP	1.444 (3) / 1.403 (3) ^[e]	1.456 / 1.406	5.9	58
<i>syn</i> -HDIP	1.443 (2) / 1.400 (2) ^[e]	1.446 / 1.407	4.2	59
<i>anti</i> -HDIP	1.444 (2) / 1.419 (2) ^[e]	1.450 / 1.423	4.1	65
DIANT	1.468 (3) / 1.406 (3) ^[f]	1.454 / 1.393	5.6	62
<i>linear</i> -DIANT	1.451 (3) / 1.397 (3) ^[g]	1.452 / 1.392	5.0	64
<i>syn</i> -DIANT	1.441 (3) / 1.391 (3) ^[g]	1.442 / 1.396	5.8	69
<i>anti</i> -DIANT	1.449 (6) / 1.412 (5) ^[g]	1.446 / 1.404	8.5	71

[a]: Taken from Haley et al., *Chem. Sci.* **2014**, *5*, 3627-3633; [b]: Taken from Chi et al., *Chem. Sci.* **2014**, *5*, 4490-4503; [c]: Taken from Haley et al., *J. Am. Chem. Soc.* **2014**, *136*, 9181–9189; [d]: Taken from Haley et al., *J. Am. Chem. Soc.* **2016**, *138*, 16827–16838; [e]: Taken from Frigoli et al., *Chem. Sci.* **2020**, *11*, 12194-12205; [f]: Taken from Haley et al., *Nat. Chem.* **2016**, *8*, 753–759; [g]: Taken from Haley et al., *Chem* **2020**, *6*, 1353–1368.

THEORITICAL CALCULATIONS

The computations were mainly performed using the computer facilities at the Research Institute for Information Technology, Kyushu University. Molecular orbital calculations were performed using the program Gaussian 16 except for the ACID (anisotropy of the induced current density) calculations and NICS calculations.^{vi} The geometries were optimized at the B3LYP/6-311G(d,p) level, and these optimized structures are used for the further calculations. The presence of energy minima for the geometry optimization was confirmed by the absence of imaginary modes (no imaginary frequencies). To numerically achieve accurate values, we have used a fine grid. We adopted two model systems, which are main aromatic backbone with or without substituents. The triisopropylsilyl (TIPS) groups were substituted with trimethylsilyl (TMS) groups. The molecular orbitals of DITT derivatives are shown in Figure S1.

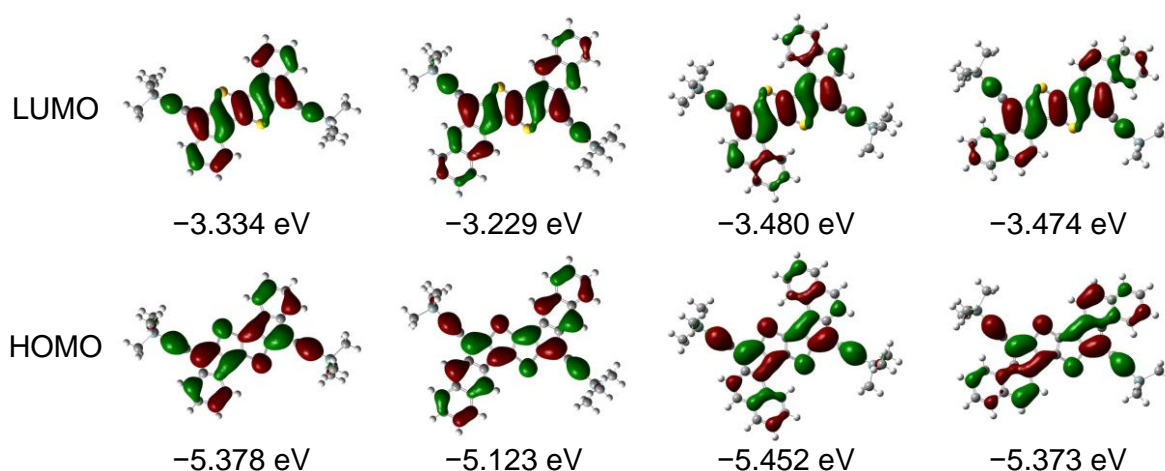


Figure S1. Molecular orbitals at the B3LYP/6-311G(d,p)

The singlet biradical factor was calculated by the natural orbital occupation number (NOON) of the LUMO in a spin-unrestricted Hartree-Fock (HF) calculation using 6-31G(d,p) basis set.^{vii} The broken symmetry UHF calculations gave LUMO occupation number. According to the Yamaguchi scheme,^{viii} the index for singlet biradical character is expressed as

$$y_i = 1 - \frac{2T_i}{1 + T_i^2}$$

where T_i is the orbital overlap between the corresponding orbital pairs and it can be presented using the NOON of HOMO and LUMO.

$$T_i = \frac{n_{HOMO} - n_{LUMO}}{2}$$

The diradical characters by the theoretical calculation are listed in Table S3.

Table S3. The biradical character γ

compounds	UHF/6-311G(d,p)
DITT	0.07
<i>linear-DITT</i>	0.07
<i>syn-DITT</i>	0.15
<i>anti-DITT</i>	0.15

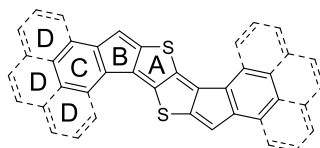
^a scf=xqc keyword

The current density plotted onto the ACID were generated using the programs Gaussian 09 and AICD 2.0.0.^{ix,x,xi} The ring current analysis was performed with the CSGT method at the B3LYP/6-311+G(d,p) level with IOp(10/93=2). The magnetic field was applied parallel to z-axis (0 0 1). The number of points of cartesian grid was set as 160000.

NICS values were estimated using the GIAO-B3LYP/6-311+G(d,p) methods and performed using Gaussian 09 and Aroma 1.0.^{xii} NICS values employ σ -only model to obtain the effect of the π contribution only, where the positive charges were used for heterocycles. NICS(0) π_{zz} , NICS(1) π_{zz} , and NICS(1.7) π_{zz} are summarized in Table S4.

Table S4. NICS(0) π_{zz} , NICS(1) π_{zz} , and NICS(1.7) π_{zz} values

DITT core				<i>linear-DITT</i> core			
Ring	NICS(0) π_{zz}	NICS(1) π_{zz}	NICS(1.7) π_{zz}	Ring	NICS(0) π_{zz}	NICS(1) π_{zz}	NICS(1.7) π_{zz}
A	7.1	4.7	2.0	A	5.3	3.4	1.7
B	16.0	12.0	3.9	B	13.2	9.3	2.8
C	-21.0	-18.4	-10.0	C	-20.6	-18.6	-10.6
				D	-28.3	-25.0	-14.2
<i>syn-DITT</i> core				<i>anti-DITT</i> core			
Ring	NICS(0) π_{zz}	NICS(1) π_{zz}	NICS(1.7) π_{zz}	Ring	NICS(0) π_{zz}	NICS(1) π_{zz}	NICS(1.7) π_{zz}
A	18.2	10.0	4.6	A	11.9	8.8	4.4
B	20.4	20.7	8.0	B	24.3	19.0	7.1
C	-24.5	-19.9	-10.8	C	-23.1	-20.7	-11.4
D	-28.5	-24.9	-14.0	D	-27.1	-24.1	-13.8



The time-dependent density functional theory (TD-DFT) calculations were conducted at the B3LYP/6-311+G(d,p) level.

Table S5. Calculated vertical excitation energies (VEE) for singlet excited states, wavelength, and oscillator strength (f) for **DITT** derivatives

DITT				linear-DITT			
Excited States	VEE (eV)	Wavelength (nm)	f	Excited States	VEE (eV)	Wavelength (nm)	f
1	1.8959	653.96	0.0000	1	1.9214	645.30	1.0454
2	1.9619	631.96	0.6138	2	2.1095	587.74	0.0000
3	2.7453	451.62	0.6353	3	2.6023	476.45	0.2200
4	3.1102	398.64	0.0000	4	2.6818	462.32	0.0000
5	3.5093	353.30	0.0007	5	3.1233	396.97	0.3208
6	3.5153	352.70	0.1958	6	3.1464	394.05	0.0000
7	3.5272	351.51	0.0002	7	3.1941	388.16	0.2036
8	3.5505	349.20	0.0000	8	3.3799	366.82	0.0000
9	3.8671	320.61	0.0000	9	3.6177	342.71	0.0001
10	4.0026	309.76	0.0000	10	3.6351	341.08	0.0002
11	4.1034	302.15	0.1926	11	3.6567	339.06	0.0000
12	4.1205	300.90	0.0000	12	3.8172	324.80	0.0000
syn-DITT				anti-DITT			
Excited States	VEE (eV)	Wavelength (nm)	f	Excited States	VEE (eV)	Wavelength (nm)	f
1	1.4224	871.66	0.0000	1	1.4505	854.74	0.0000
2	1.6690	742.86	0.1648	2	1.5832	783.11	0.2170
3	2.1868	566.96	0.7598	3	2.4160	513.17	1.2253
4	2.8429	436.12	0.0000	4	2.6572	466.60	0.0000
5	2.9849	415.37	0.0000	5	2.8751	431.23	0.0759
6	3.1757	390.42	0.2231	6	3.1954	388.00	0.0000
7	3.3425	370.93	0.0002	7	3.3556	369.49	0.0002
8	3.4067	363.94	0.0003	8	3.3699	367.91	0.0000
9	3.4222	362.29	0.0000	9	3.3722	367.67	0.0000
10	3.4958	354.67	0.0000	10	3.5862	345.73	0.0000
11	3.5328	350.95	0.0275	11	3.7113	334.08	0.1047
12	3.6526	339.44	0.3355	12	3.7953	326.68	0.0060

Table S6. Calculated vertical excitation energies (VEE) for singlet excited states, wavelength, and oscillator strength (f) for IF derivatives

IF				linear-IF			
Excited States	VEE (eV)	Wavelength (nm)	f	Excited States	VEE (eV)	Wavelength (nm)	f
1	1.7746	698.65	0.0000	1	1.9260	643.73	0.8220
2	2.0651	600.39	0.6808	2	1.9741	628.06	0.0000
3	3.2005	387.39	0.0430	3	2.6240	472.51	0.0000
4	3.2087	386.39	0.0000	4	2.7307	454.05	0.0000
5	3.2642	379.83	0.0000	5	2.7920	444.07	0.0858
6	3.4146	363.10	0.0000	6	3.2965	376.11	0.2841
7	3.4421	360.20	0.0004	7	3.4266	361.83	0.0558
8	3.4825	356.02	0.3456	8	3.5012	354.11	0.0000
9	3.6549	339.23	0.0002	9	3.5273	351.50	0.0001
10	4.0219	308.27	1.0599	10	3.6117	343.29	1.4776
11	4.3718	283.60	0.1600	11	3.6621	338.56	0.0002
12	4.4181	280.63	0.0001	12	3.8496	322.07	0.0000
syn-IF				anti-IF			
Excited States	VEE (eV)	Wavelength (nm)	f	Excited States	VEE (eV)	Wavelength (nm)	f
1	1.2984	954.87	0.0000	1	1.2932	958.77	0.0000
2	1.8466	671.44	0.4288	2	1.7504	708.32	0.5802
3	2.3435	529.05	0.1195	3	2.5867	479.32	0.2392
4	2.8962	428.10	0.0000	4	2.6338	470.74	0.0000
5	3.0503	406.46	0.0000	5	2.9710	417.32	0.0236
6	3.1998	387.48	0.2938	6	3.1587	392.51	0.0000
7	3.2114	386.08	0.0000	7	3.2497	381.52	0.0000
8	3.3315	372.16	0.0003	8	3.2873	377.16	0.0003
9	3.3697	367.94	0.0000	9	3.4226	362.25	0.0000
10	3.3961	365.08	0.9563	10	3.5648	347.80	0.0002
11	3.5283	351.40	0.0000	11	3.6162	342.86	0.4977
12	3.7364	331.83	0.1623	12	3.6534	339.36	0.0023

The transfer integrals are computed by using DFT with the PW91/TZVP in the Gaussian 16. The reorganization energies (λ) were calculated by using the adiabatic potential-energy surfaces method at the B3LYP/6-311+G(d,p). The theoretical drift mobilities were calculated based on the classical Marcus-Hush theory.^{xiii}

OFETs

Bottom-gate/top-contact (BG/TC) OFETs were constructed on heavily doped n-type silicon wafers covered with thermally grown silicon dioxide (300 nm) which was cleaned by piranha solution. The silicon dioxide acts as a gate dielectric layer, and the silicon wafer serves as a gate electrode. The cross-linked PVP (poly-4-vinylphenol) was prepared by spin-coating from a solution of PVP (Aldrich 436224, $M_w \sim 25,000$, 1.0 wt%) and poly(melamine-co-formaldehyde) ($M_n \sim 432$, 1.0 wt%) in propylene glycol monomethyl ether acetate (PGMEA) at the rotational speed of 500 rpm for 5 s and then 4000 rpm for 60 s, followed by the cross-linkage at temperatures of 150 °C for 60 min under nitrogen atmosphere. Organic semiconductor layers were formed by drop-casting (see Figure S5) from a 0.1~0.2 wt% solution of HDIP derivatives with 1/4 wt% polystyrene (PS) in *o*-dichlorobenzene at 60 °C, followed by thermal annealing at 60 °C for ca. 30 min. Top-contact gold source-drain electrodes (50 nm) were deposited on PVP through a shadow mask with $L = 50, 100, 150$ and $200 \mu\text{m}$, and $W = 2000 \mu\text{m}$.

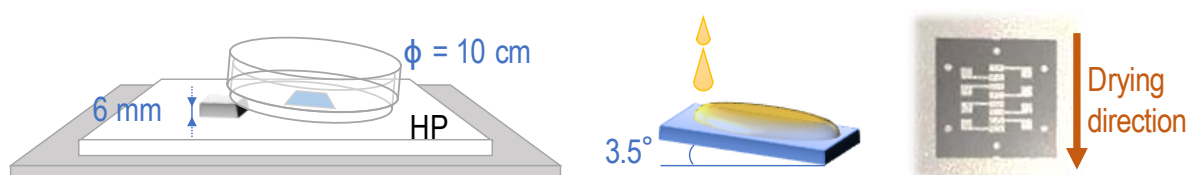


Figure S2. Schematic image of the drop-casting procedure. The substrates were placed inside the petri-dish with the saturated solvent vapor at 60 °C, then 30 μL of the semiconductor solution was drop-casted.

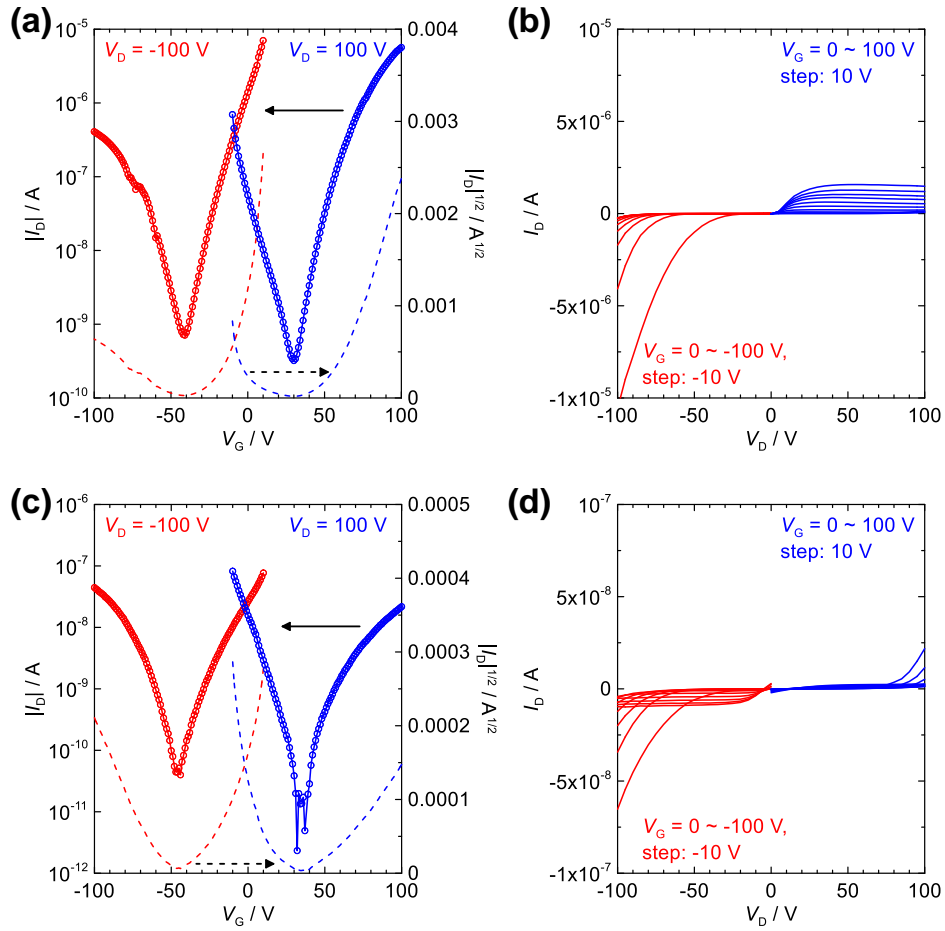


Figure S3. (a) Transfer and (b) output characteristics of *syn-DITT*. (c) Transfer and (d) output characteristics of *anti-DITT*.

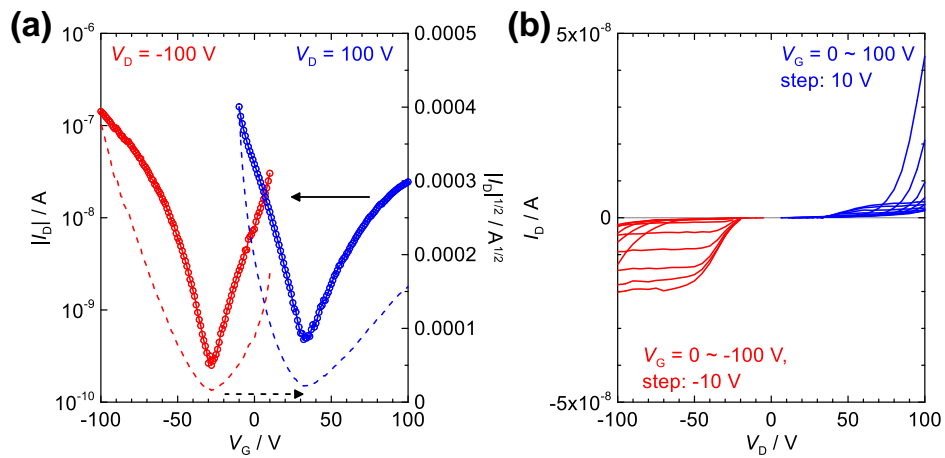


Figure S4. (a) Transfer and (b) output characteristics of *linear-IF*.

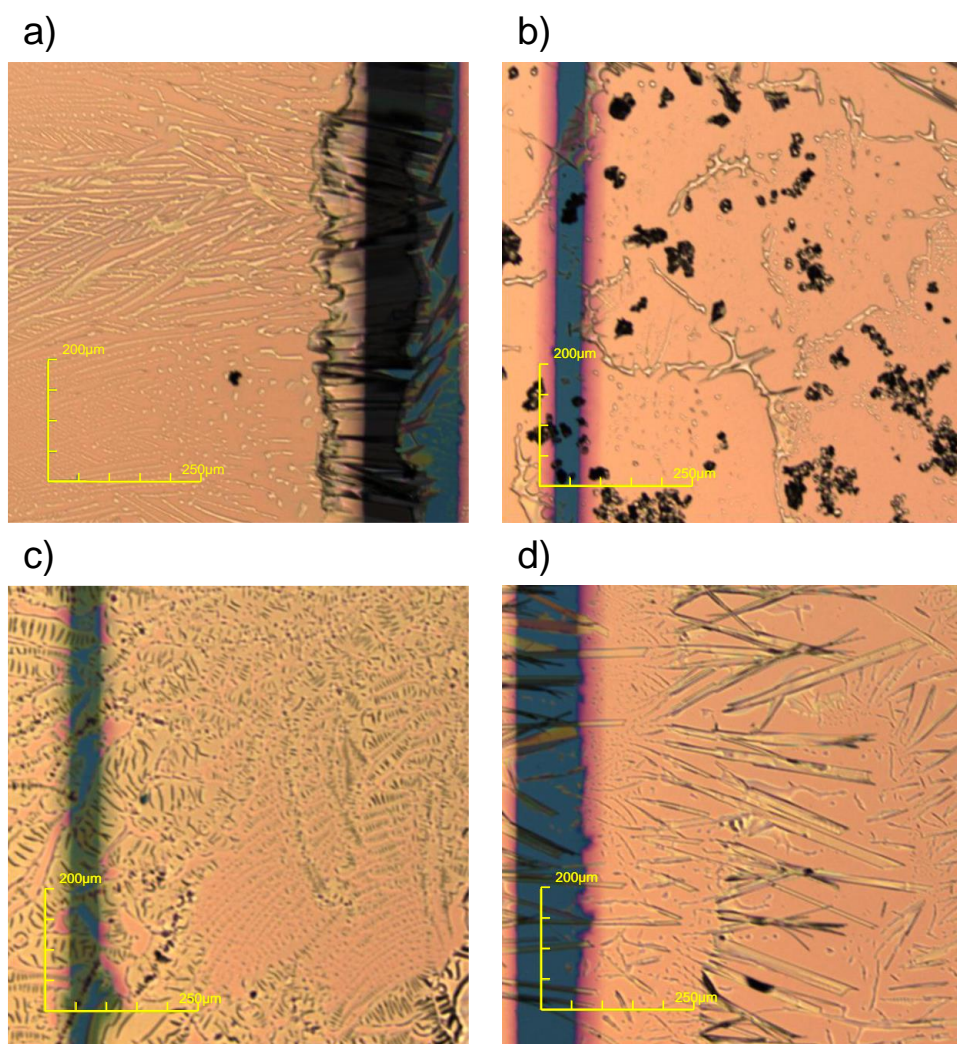
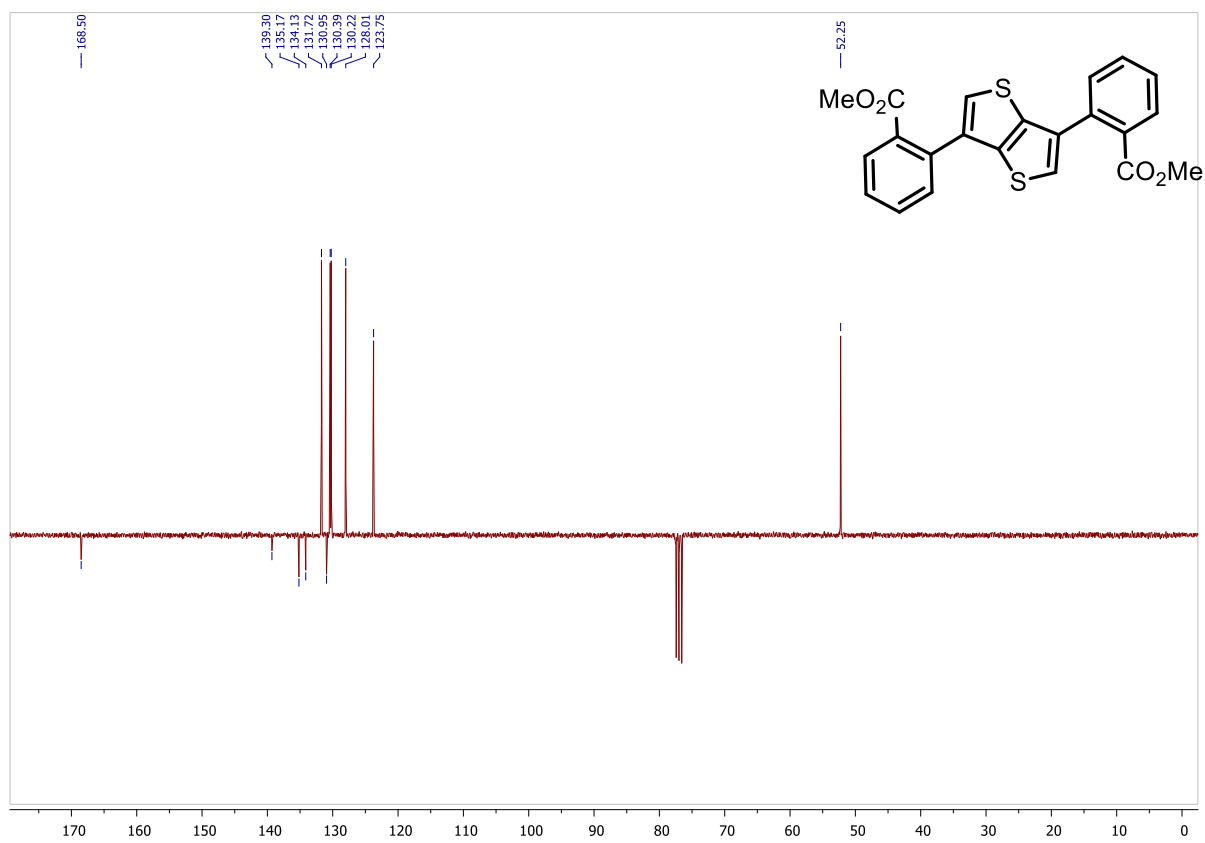
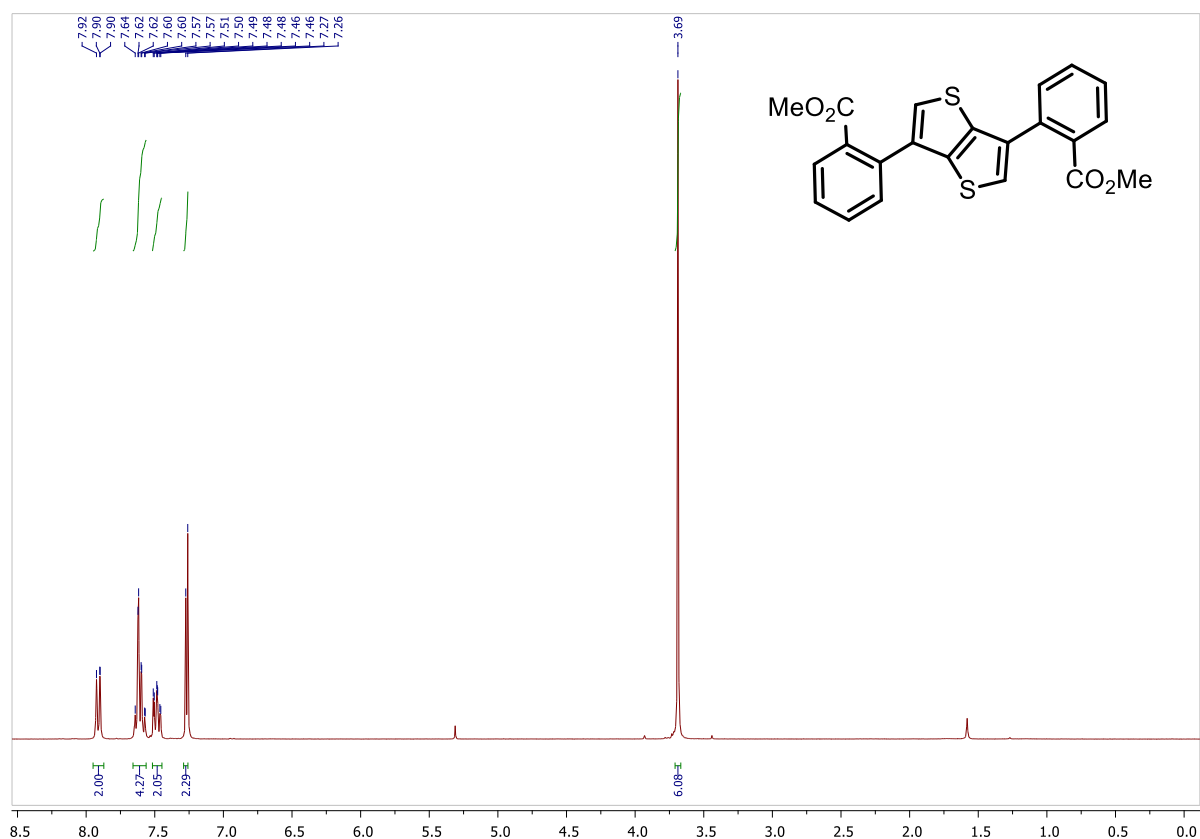
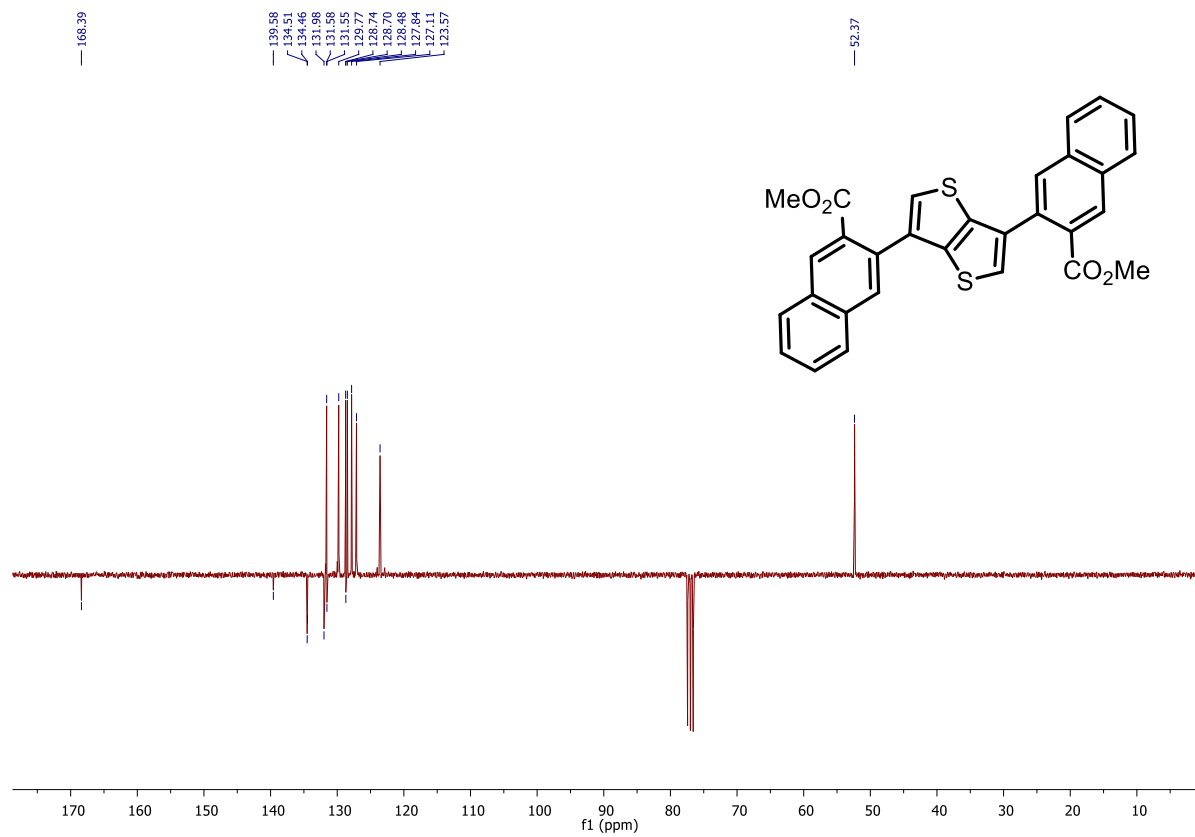
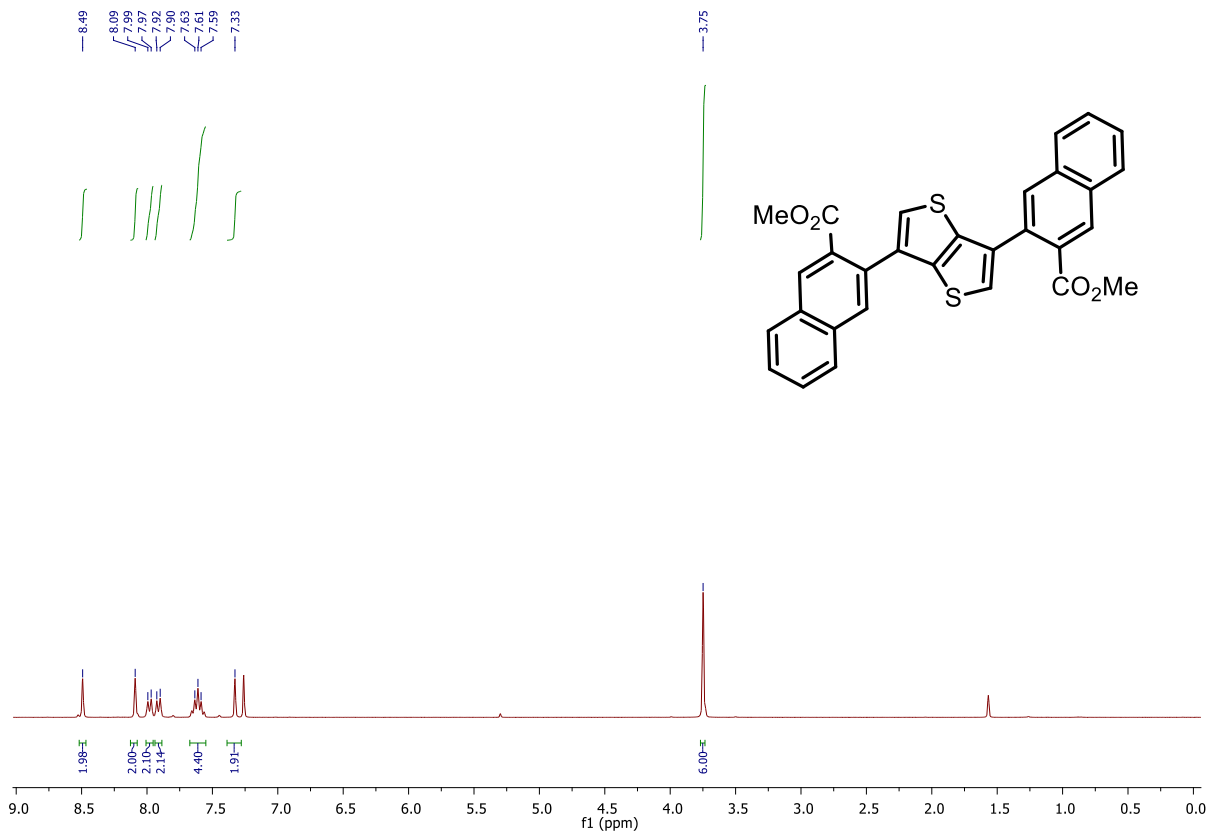
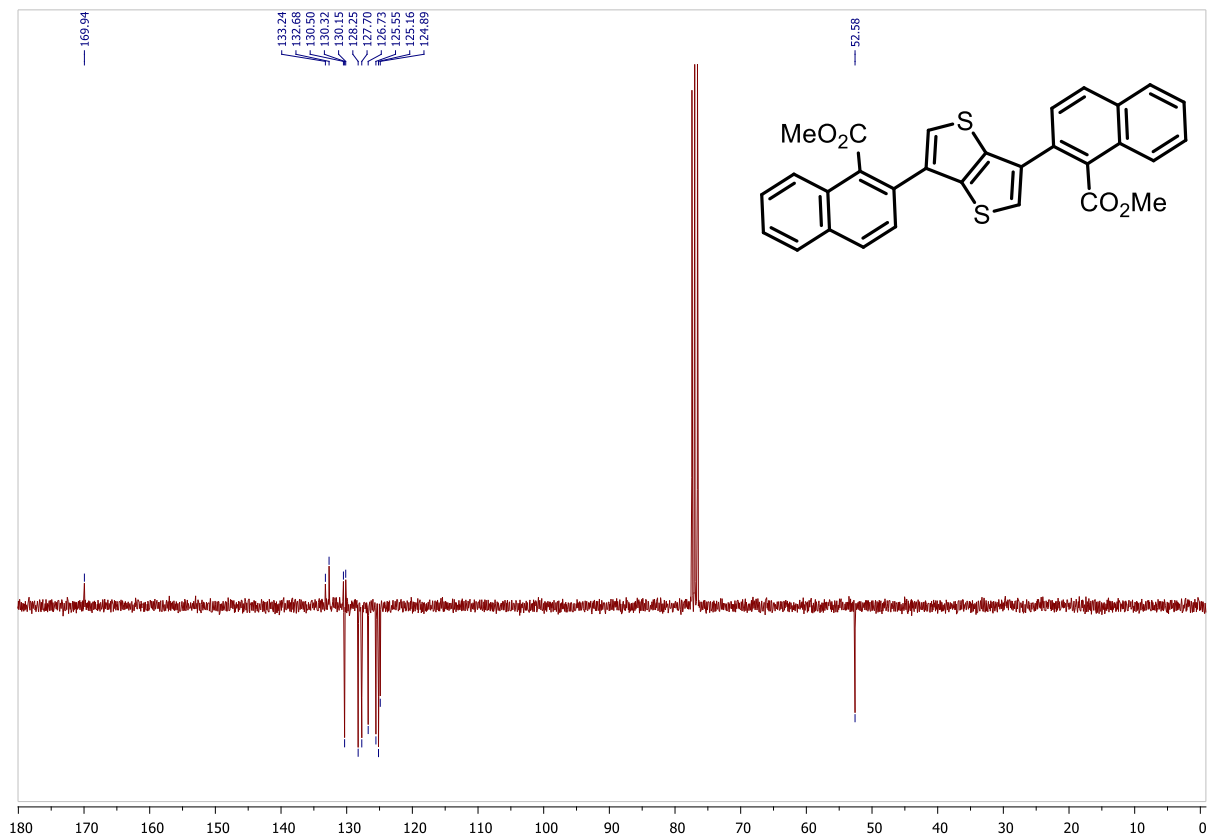
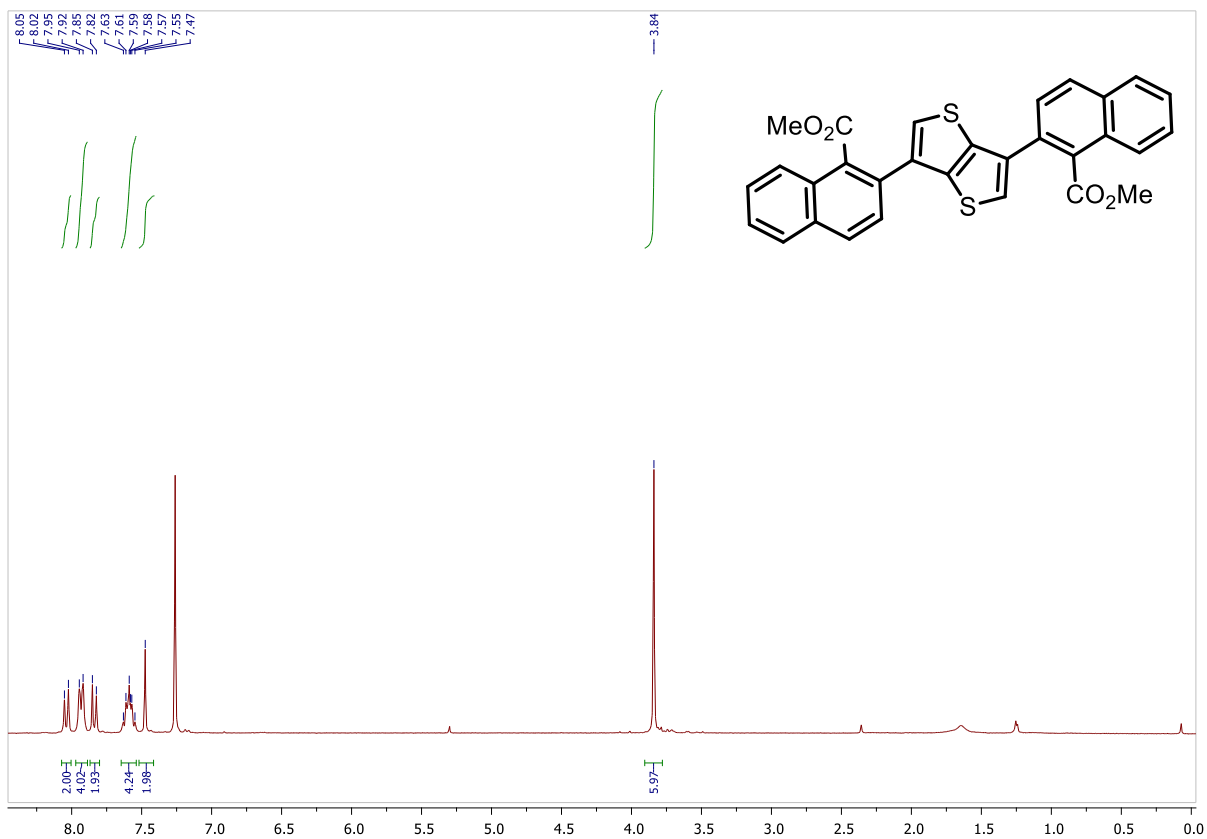


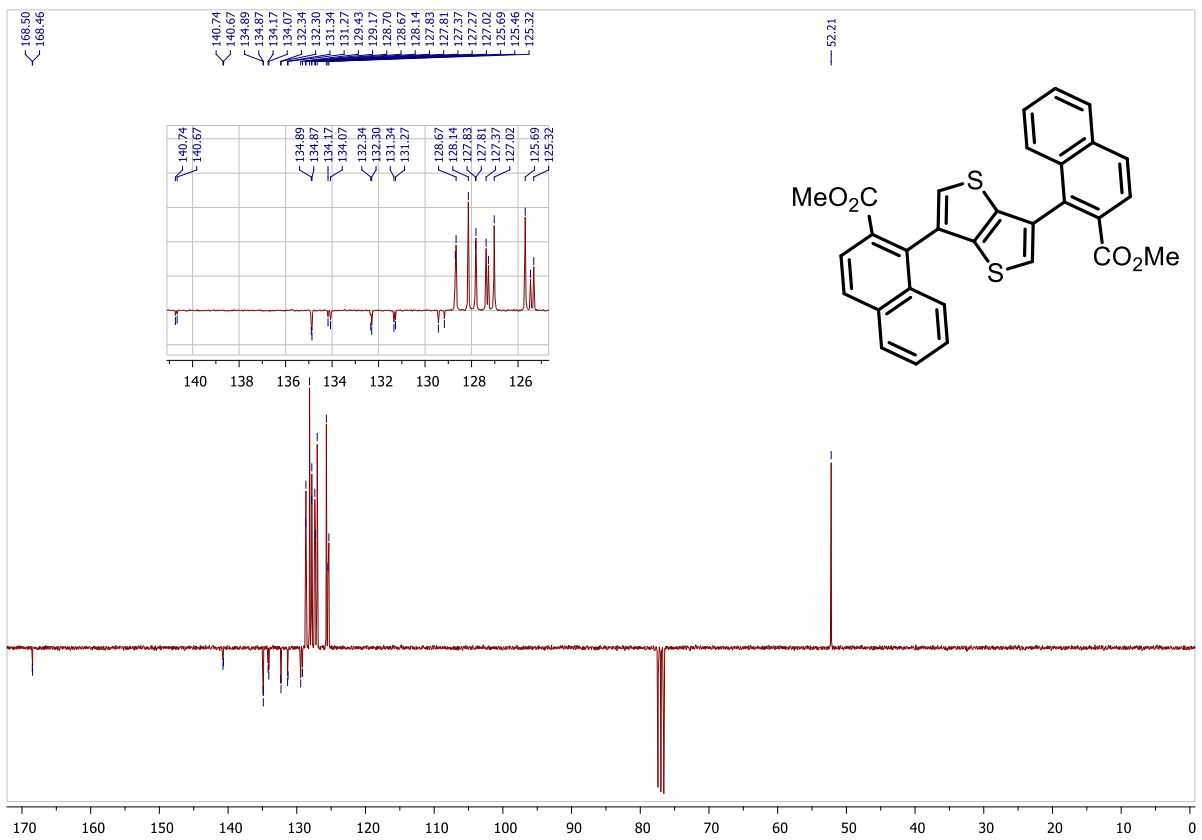
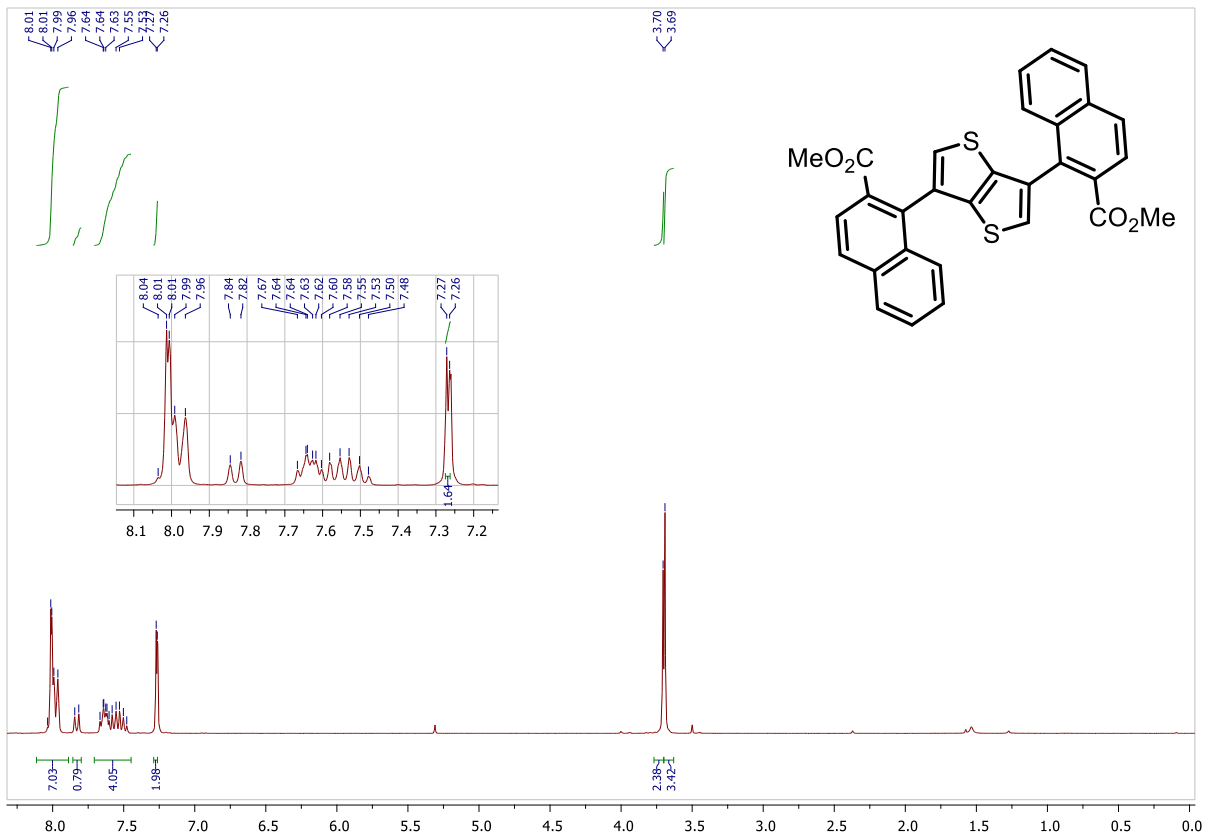
Figure S5. Microscope images for thin-films prepared by drop-casting of a) DITT, b) *linear*-DITT, c) *syn*-DITT and d) *anti*-DITT.

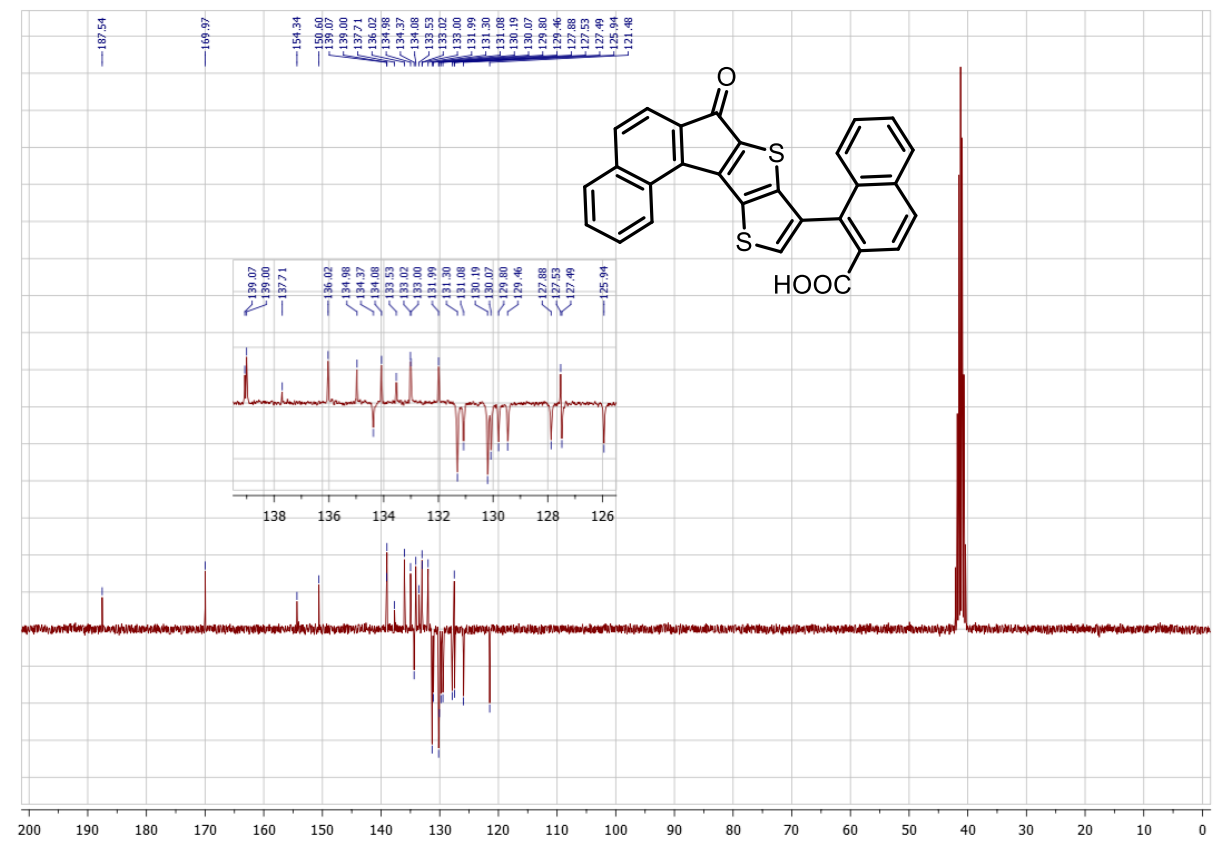
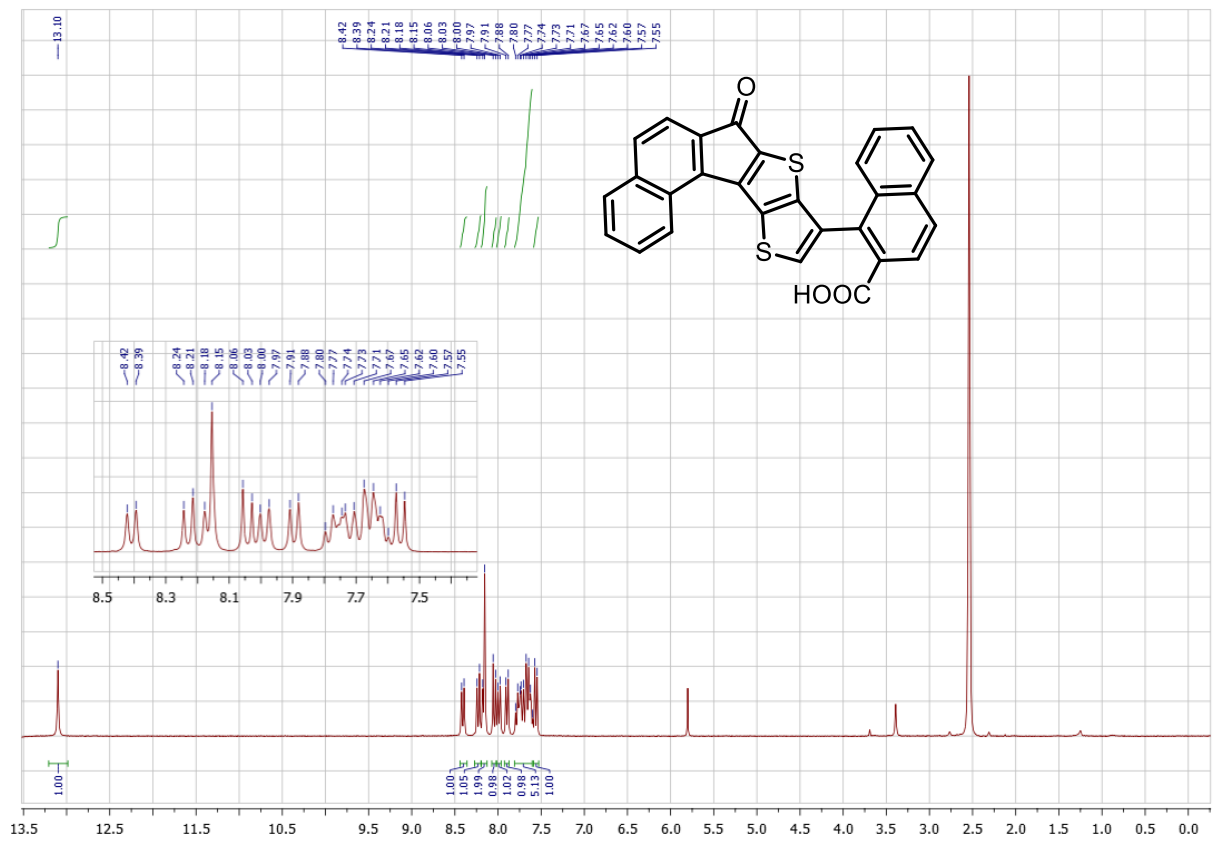
RMN SPECTRA

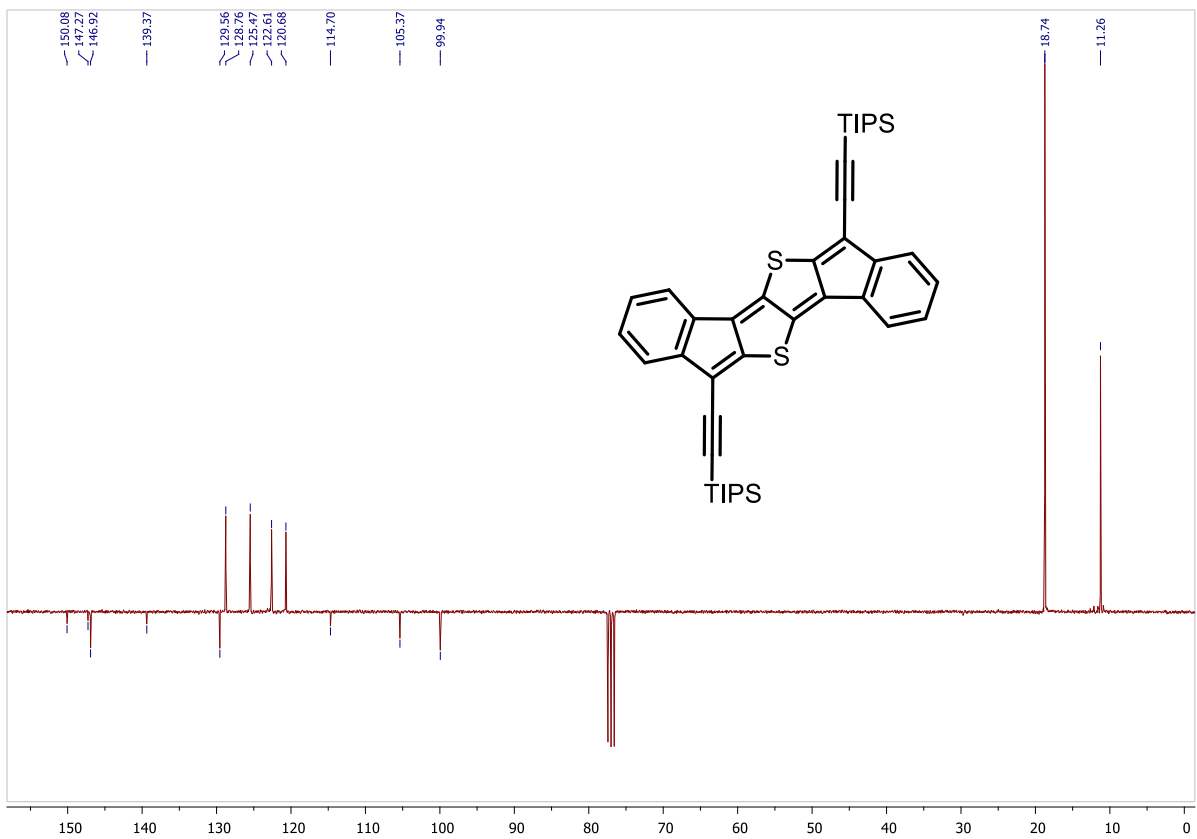
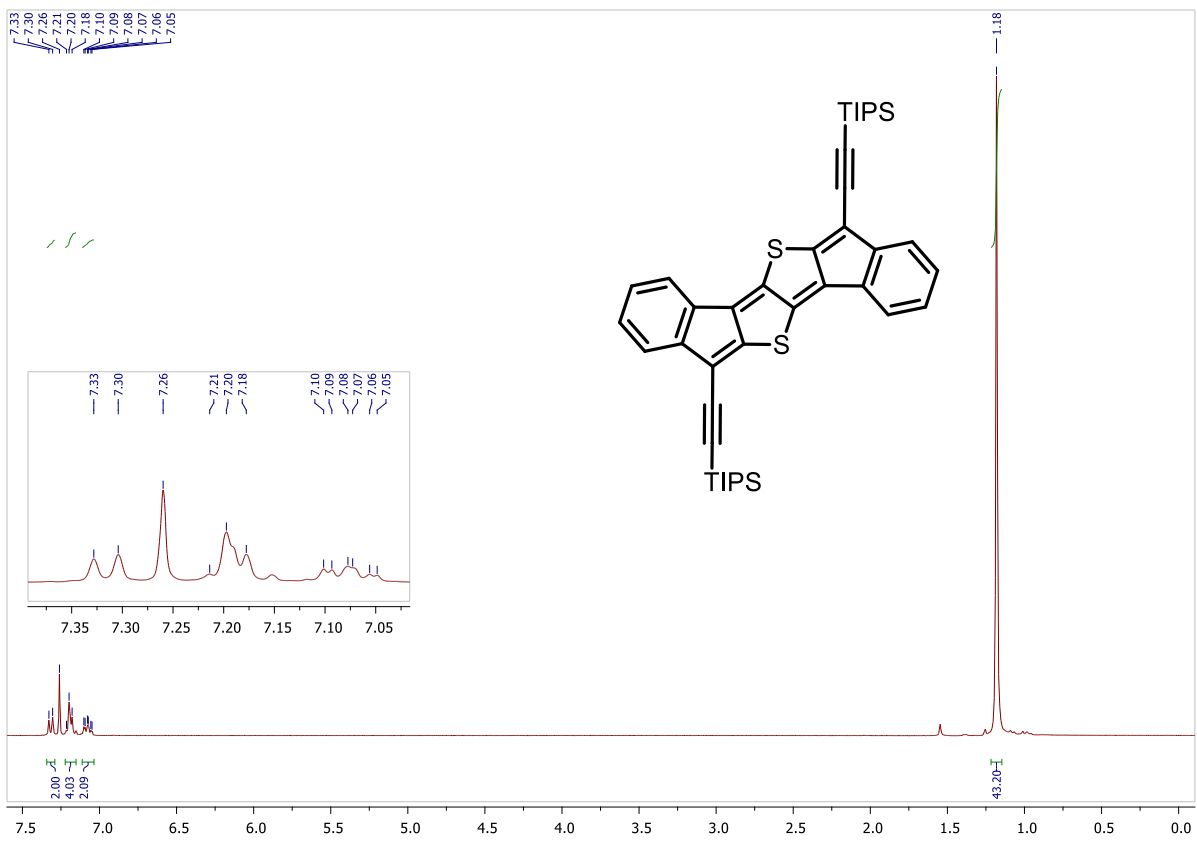


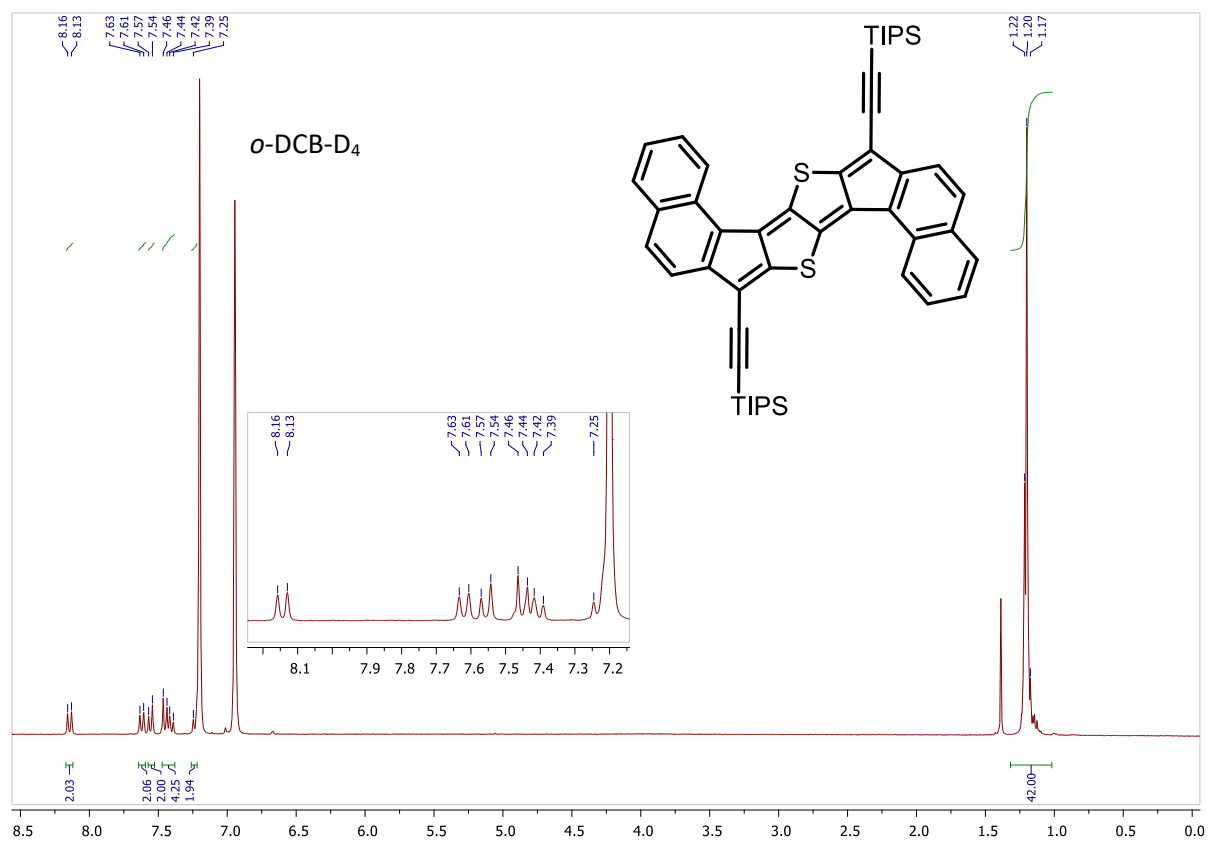
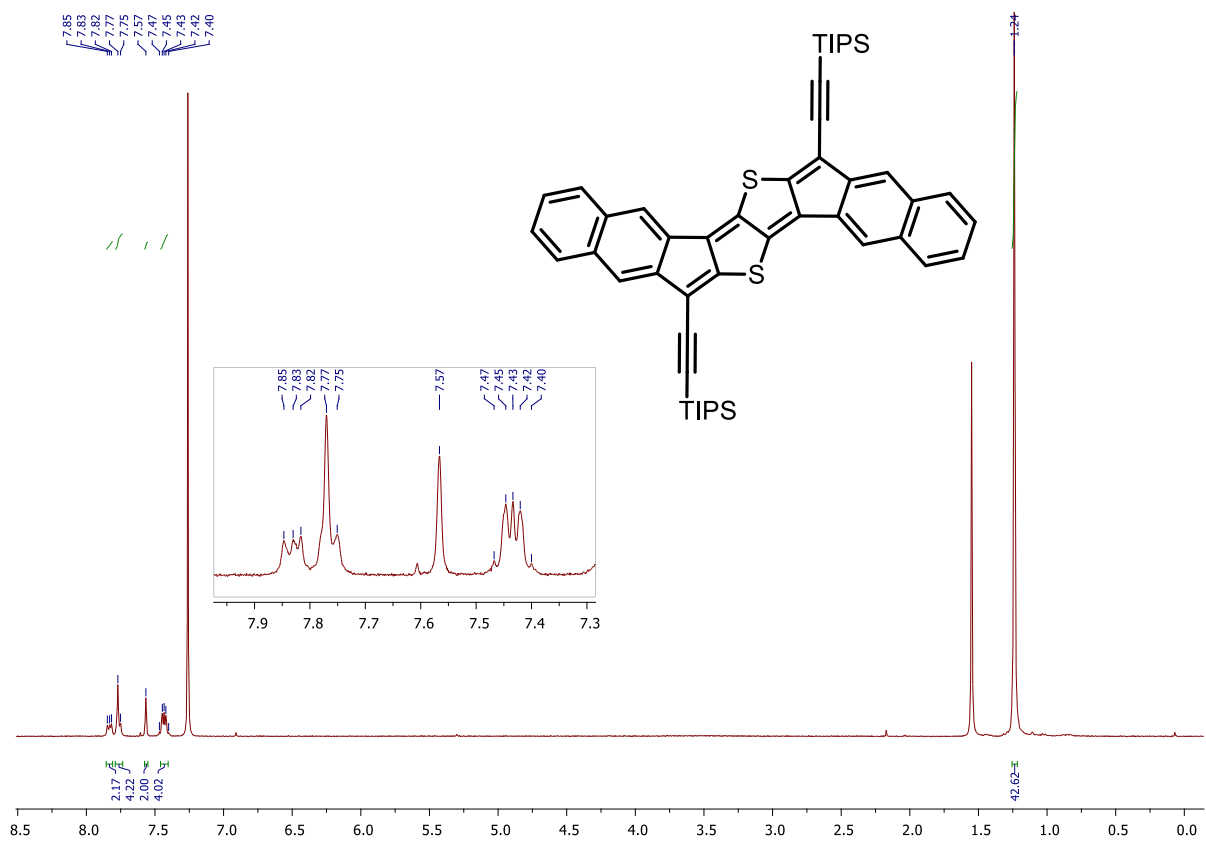


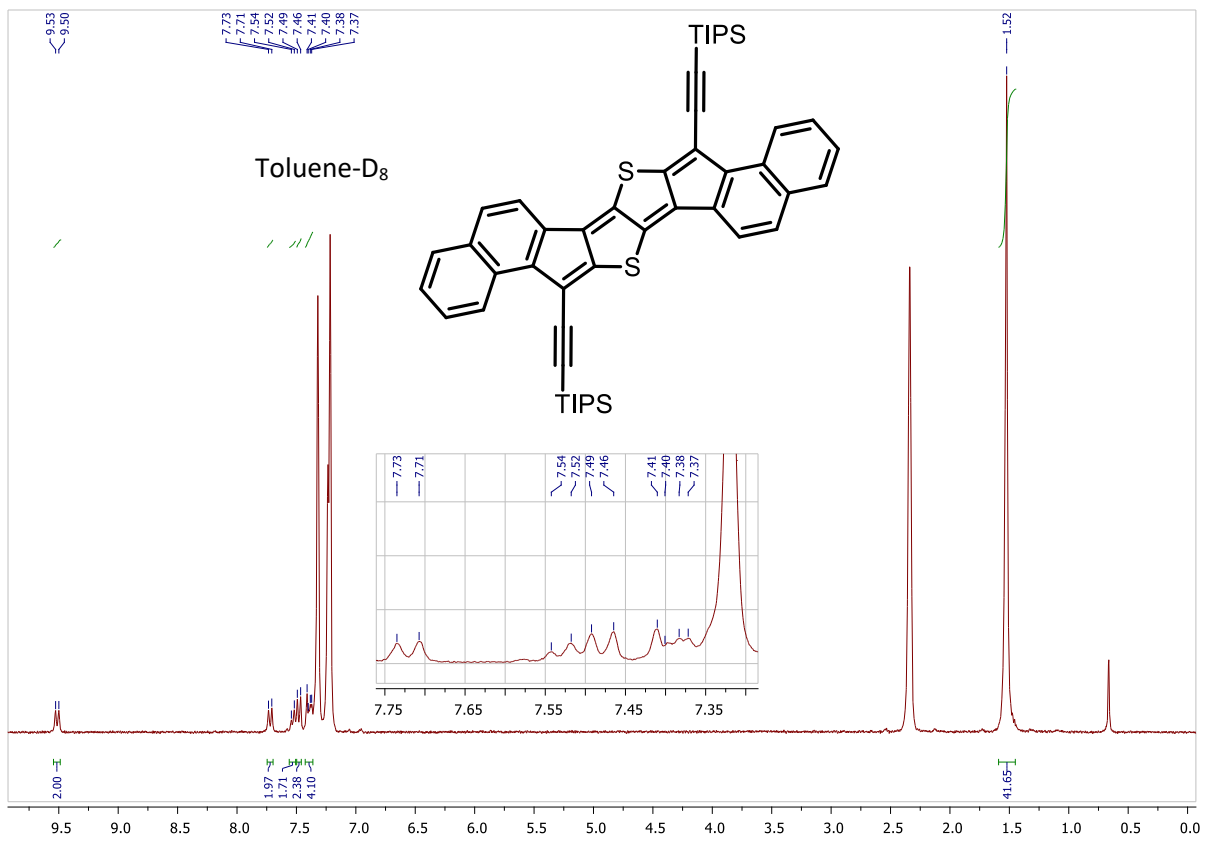




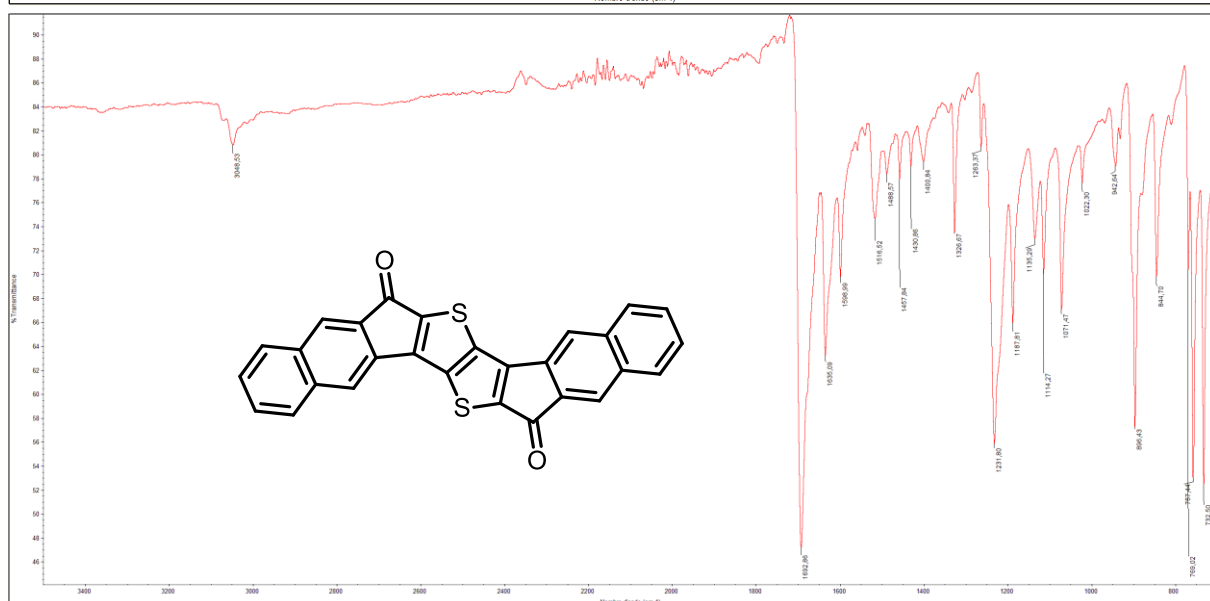
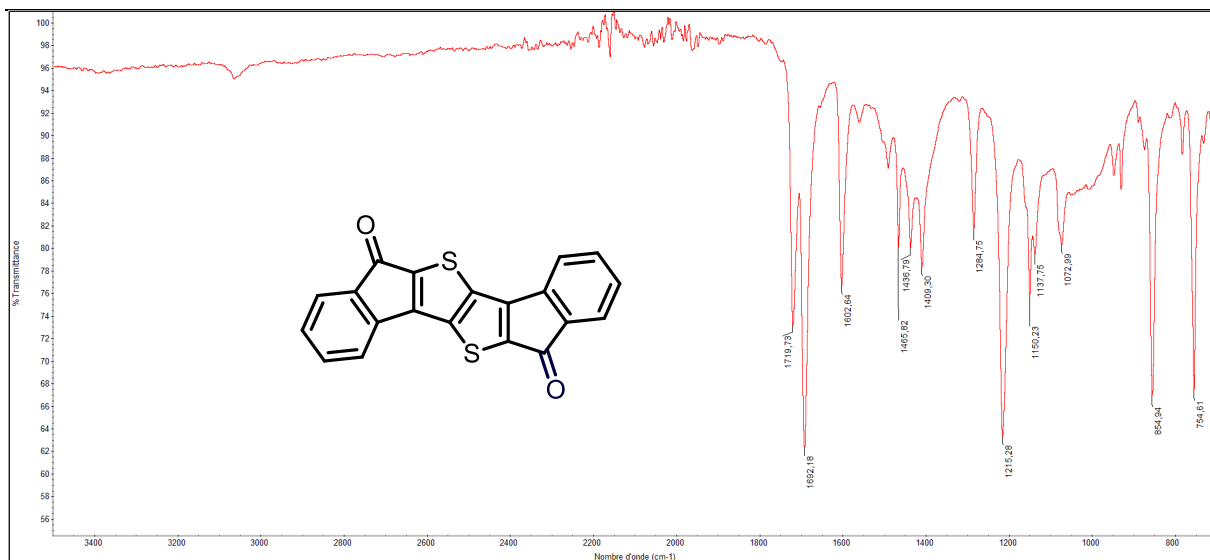


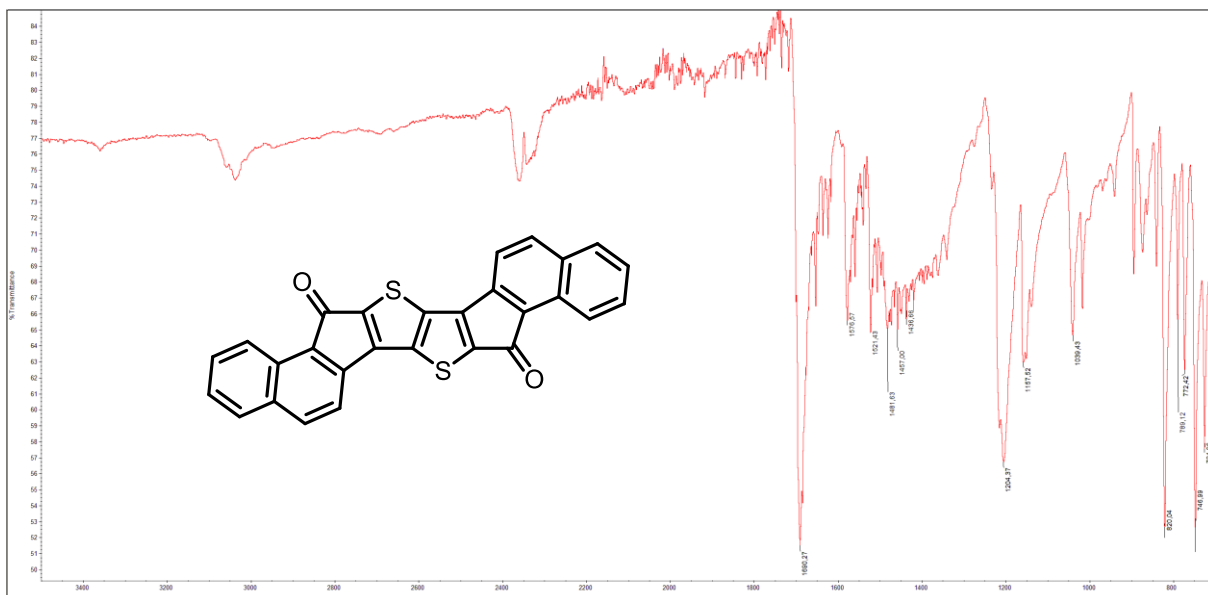
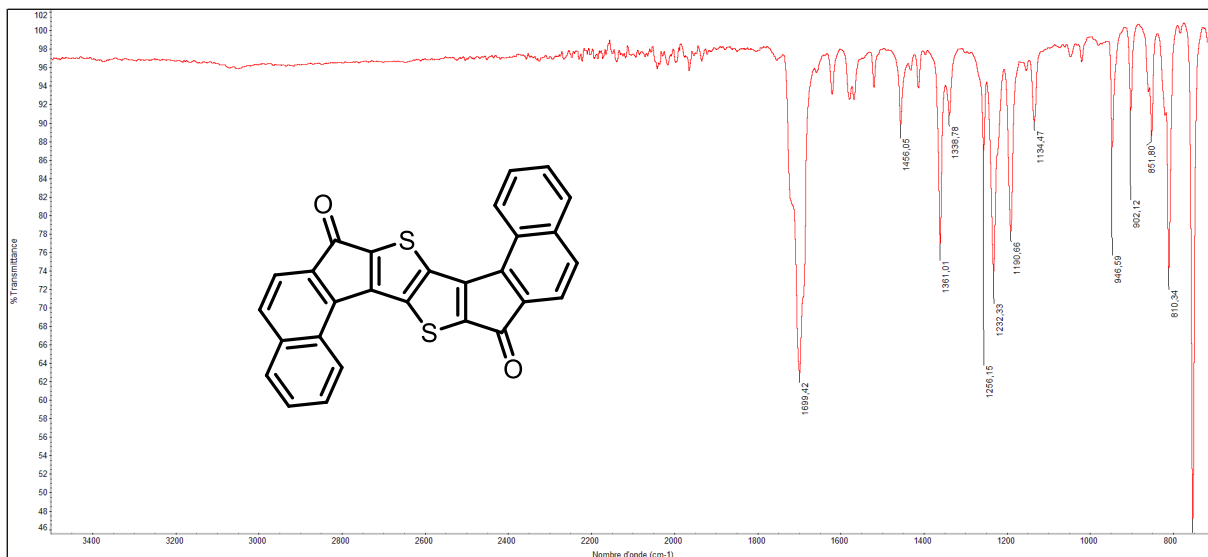






INFRARED SPECTRA





REFERENCES

- ⁱ J. Lee and J. Park, *Org. Lett.*, 2015, **17**, 3960–3963.
- ⁱⁱ L. Ling, Y. He, X. Zhang, M. Luo and X. Zeng, *Angew. Chem. Int. Ed.*, 2019, **58**, 6554–6558.
- ⁱⁱⁱ Y. Xia, Z. Liu, Q. Xiao, P. Qu, R. Ge, Y. Zhang and J. Wang, *Angew. Chem. Int. Ed.*, 2012, **51**, 5714–5717.
- ^{iv} F. Krätzschar, M. Kaßel, D. Delony and A. Breder, *Chem. Eur. J.*, 2015, **21**, 7030–7034.
- ^v B. Ghaffari, S. M. Preshlock, D. L. Plattner, R. J. Staples, P. E. Maligres, S. W. Krska, R. E. Maleczka and M. R. Smith, *J. Am. Chem. Soc.*, 2014, **136**, 14345–14348.
- ^{vi} Gaussian 16, Revision A.03, Frisch, M. J.; Trucks, G. W.; Schlegel, H. B.; Scuseria, G. E.; Robb, M. A.; Cheeseman, J. R.; Scalmani, G.; Barone, V.; Petersson, G. A.; Nakatsuji, H.; Li, X.; Caricato, M.; Marenich, A. V.; Bloino, J.; Janesko, B. G.; Gomperts, R.; Mennucci, B.; Hratchian, H. P.; Ortiz, J. V.; Izmaylov, A. F.; Sonnenberg, J. L.; Williams-Young, D.; Ding, F.; Lipparini, F.; Egidi, F.; Goings, J.; Peng, B.; Petrone, A.; Henderson, T.; Ranasinghe, D.; Zakrzewski, V. G.; Gao, J.; Rega, N.; Zheng, G.; Liang, W.; Hada, M.; Ehara, M.; Toyota, K.; Fukuda, R.; Hasegawa, J.; Ishida, M.; Nakajima, T.; Honda, Y.; Kitao, O.; Nakai, H.; Vreven, T.; Throssell, K.; Montgomery, J. A., Jr.; Peralta, J. E.; Ogliaro, F.; Bearpark, M. J.; Heyd, J. J.; Brothers, E. N.; Kudin, K. N.; Staroverov, V. N.; Keith, T. A.; Kobayashi, R.; Normand, J.; Raghavachari, K.; Rendell, A. P.; Burant, J. C.; Iyengar, S. S.; Tomasi, J.; Cossi, M.; Millam, J. M.; Klene, M.; Adamo, C.; Cammi, R.; Ochterski, J. W.; Martin, R. L.; Morokuma, K.; Farkas, O.; Foresman, J. B.; Fox, D. J. Gaussian, Inc., Wallingford CT, **2016**.
- ^(vii) D. Doehnert and J. Koutecký, *J. Am. Chem. Soc.* **1980**, *102*, 1789–1796.
- ^(viii) Yamaguchi, K. *Chem. Phys. Lett.* **1975**, *33*, 330–335.
- ^{ix} (a) Herges, R.; Geuenich, D. Delocalization of Electrons in Molecules. *J. Phys. Chem. A* **2001**, *105*, 3214; (b) Geuenich, D.; Hess, K.; Kohler, F.; Herges, R. Anisotropy of the Induced Current Density (ACID), a General Method To Quantify and Visualize Electronic Delocalization. *Chem. Rev.* **2005**, *105*, 3758.
- ^x Gaussian 09, Revision D.01, Frisch, M. J.; Trucks, G. W.; Schlegel, H. B.; Scuseria, G. E.; Robb, M. A.; Cheeseman, J. R.; Scalmani, G.; Barone, V.; Mennucci, B.; Petersson, G. A.; Nakatsuji, H.; Caricato, M.; Li, X.; Hratchian, H. P.; Izmaylov, A. F.; Bloino, J.; Zheng, G.; Sonnenberg, J. L.; Hada, M.; Ehara, M.; Toyota, K.; Fukuda, R.; Hasegawa, J.; Ishida, M.; Nakajima, T.; Honda, Y.; Kitao, O.; Nakai, H.; Vreven, T.; Montgomery, J. A., Jr.; Peralta, J. E.; Ogliaro, F.; Bearpark, M.; Heyd, J. J.; Brothers, E.; Kudin, K. N.; Staroverov, V. N.; Kobayashi, R.; Normand, J.; Raghavachari, K.; Rendell, A.; Burant, J. C.; Iyengar, S. S.; Tomasi, J.; Cossi, M.; Rega, N.; Millam, J. M.; Klene, M.; Knox, J. E.; Cross, J. B.; Bakken, V.; Adamo, C.; Jaramillo, J.; Gomperts, R.; Stratmann, R. E.; Yazyev, O.; Austin, A. J.; Cammi, R.; Pomelli, C.; Ochterski, J. W.; Martin, R. L.; Morokuma, K.; Zakrzewski, V. G.; Voth, G. A.; Salvador, P.; Dannenberg, J. J.; Dapprich, S.; Daniels, A. D.; Farkas, Ö.; Foresman, J. B.; Ortiz, J. V.; Cioslowski, J.; Fox, D. J. Gaussian, Inc., Wallingford CT, **2009**.
- ^{xi} Keith, T. A.; Bader, R. F. W. Calculation of magnetic response properties using a continuous set of gauge transformations. *Chem. Phys. Lett.* **1993**, *210*, 223.
- ^{xii} (a) Rahalkar, A. Stanger, Aroma: <http://chemistry.technion.ac.il/members/amnon-stanger/>; (b) Stanger, A. Nucleus-Independent Chemical Shifts (NICS): Distance Dependence and Revised Criteria for Aromaticity and Antiaromaticity. *J. Org. Chem.* **2006**, *71*, 883; (c) Stanger, A. Obtaining Relative Induced Ring Currents Quantitatively from NICS. *J. Org. Chem.* **2010**, *75*, 2281; (d) Gershoni-Poranne, R.; Stanger, A. The NICS-XY-Scan: Identification of Local and Global Ring Currents in Multi-Ring Systems. *Chem. Eur. J.* **2014**, *20*, 5673.
- ^{xiii} (a) R. A. Marcus, *J. Chem. Phys.*, 1956, **24**, 966; (b) N. S. Hush, *J. Chem. Phys.*, 1958, **28**, 962.